The Effects of Glucose and AGEs on Skeletal Muscle and Coculture Cells (Muscle-Nerve):

Novel Model for Investigating Diabetic Myopathy and Neuropathy

Manchester Metropolitan University

The School of Healthcare Science

Manchester Metropolitan University

Razan Ahmad Alomosh
ID number :17022526
Supervisory team: Dr Nasser Al-Shanti, Dr Nessar Ahmed

MSc Biomedical Science

September 2018

Acknowledgments

Foremost, I would like to express my sincere gratitude and appreciation to my mentor-supervisor Dr. Nasser Al-Shanti for his continues support, guidance and motivation throughout my masters and my thesis. I can't imagine doing so without him being here to always support and challenge me to get the best out of me, Dr. Nasser indeed has invested in me and helped me to develop personally and professionally. He made it a memorable experience and I'll cherish this experience wherever I end up in my life. Working with Dr. Nasser and his team made me feel like I am home with my family.

Another, special gratitude to Jasdeep Saini and Marwah Abd Al Samid for all their hard work, patience and support in the lab. Another special thank you note goes to my friend and partner in this project Samantha Roe for being with me in thick and thin.

Last but not the least, I would like to thank the most important people in my life my parents, my brother Khaldun and my sister Shoroq for supporting me throughout this year and helping me to make this dream comes true.

Abstract

Background: Glucose and advanced glycation products (AGEs) are known to play a crucial role in the development of diabetic myopathy and neuropathy, which are clinically characterised by nerve damage leading to muscle weakness and wasting. The potential mechanisms of underlying nerve damage and muscle wasting linked to diabetes are not well understood and needs further investigations.

Aim: To investigate the effects of glucose and AGEs *in vitro* on human skeletal muscle monoculture and coculture (muscle-nerve) neuromuscular junction (NMJ) model.

Methods: Young Skeletal muscle cell (SkMC) line were expanded and differentiated (monoculture), and then they were treated for 96 hours with (5-15 mM/ml) D-glucose and (50-200 μg/ml) of AGEs to determine any myogenic variation between different treatments. Human SkMC was cocultured with neural progenitor cells (NPCs) which then differentiated into motor neurons. Coculture was treated with AGEs for 7 days and neurons axonal length was measured. Further, the mitochondrial bioenergetics of SkMC and NPCs were analysed using a Seahorse Bioscience XFp analyser.

Results: Significant difference were observed between the control and different glucose and AGEs treatments in terms of differentiation parameters (fusion index, myotube area and aspect ratio) over 96 hours. Both mono and coculture showed myotubes abnormal differentiation with distinct increase in myotube area and centrally clustered nuclei in treated cultures. In NMJs system, less differentiation of motor neurons with shorter axonal formation was significant ($P<0.0001$). Both models showed significant difference in some of OCR parameters following AGEs treatment compared to the control.

Conclusion: Employment of this novel human-based platform to study the effect of glucose and AGEs in inducing diabetic myopathy and neuropathy revealed abnormal differentiation of myotubes, centralised nuclei clumping, decreased axonal length of motor neurons and mitochondrial dysfunction under *in vitro* diabetic conditions. This proves the potential involvement of glucose and AGEs in inducing diabetic complications.

Contents

List of Figures

MSc Biomedical Science Dissertation Declaration 2018

'With the exception of any statements to the contrary, all the data presented in this report are the results of my own efforts and have not previously been submitted in candidature for any other degree or diploma. In addition, no parts of this report have been copied from other sources. I understand that any evidence of plagiarism and/or the use of unacknowledged third-party data will be dealt with as a very serious matter.'

Date 13 September 2018

Student name Razan Ahmad Alomosh

Student Signature RAZAN

1. Introduction

1.1 Skeletal muscle and myogenesis

Skeletal muscle makes up 40%-50% of the mass of the body, it consists of a specialized tissue comprised of muscle fibres which are multi-nucleated and non-dividing, created within embryogenesis from muscle precursor cells (Shadrach and Wagers, 2011). In addition, the muscle precursor cells produce stem cells that are specifically create muscle known as satellite cells (SC). The aptitude of muscle fibre to regenerate is based on SC of specific tissue (Bentzinger et al., 2012). The embryonic satellite cells or muscle stem cells undergo extensive proliferation in order to create enough cells and a particular number of myofibrils (Bentzinger et al., 2012). The produced myoblast from satellite cells exit the cell cycle and joins together to create multinucleated myotubes, ultimately developing into myofibres (Le Grand and Rudnicki, 2007; Zammit et al., 2004). Following the embryonic myogenesis, the differentiated myofibres are unable to proliferate any longer, and the embryonic satellite cells stay in a dormant condition awaiting stimulation for later reconstruction or regeneration of muscle (Summarised in figure 1) (Chal and Pourquié, 2017). This sequence portrays that a person has a set quantity of muscle fibres which is mainly established prior to birth and may only decrease as the fibres are lost due disease and age (Grounds, 1998).

Skeletal Muscle Myogenesis

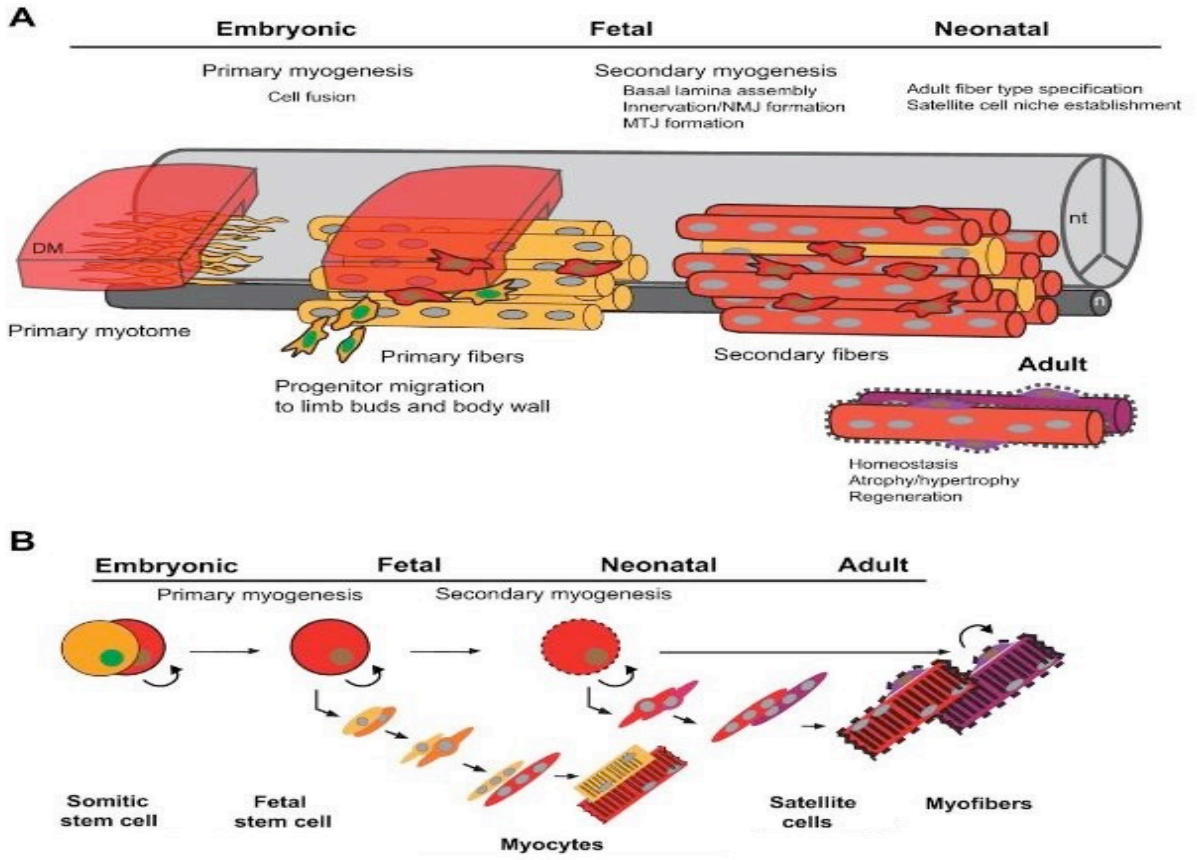

Figure 1: Stages of skeletal myogenesis from the embryo to the adult

(A) Developmental sequence of muscle formation from the dermomyotome. The early myotome (left) is composed of primary myocytes, which are aligned along the anteroposterior axis and span each somitic compartment. During secondary myogenesis (right), Pax7+ myogenic progenitors (red cytoplasm, brown nuclei) contribute to secondary (red) fibre formation, using the primary fibres as a scaffold contributing to the growth off skeletal muscles. During this phase, satellite cell precursors (purple cytoplasm, brown nuclei) localize under the basal lamina (dotted line) of the fibres where they can be found in adult muscles. processes associated with each stage are listed above. nt, neural tube; n, notochord; DM, dermomyotome; MTJ, myotendinous junction; NMJ, neuromuscular junction. (B) Differentiation of somitic progenitors to skeletal muscles and adult satellite cells. Myogenic stem cells contribute to fetal myogenesis while maintaining a pool of progenitors, which eventually become located on mature myofibers in the satellite cell niche (Chal and Pourquié, 2017).

Myogenesis can be divided into two separate sequences (Floyd et al., 2001): myoblast proliferation that takes place by means of a sequence of occurrences organized in an exact sequence, that is, cell cycle, and differentiation regarding the cells which exit a cell sequence within G1 phase and are incapable of entering it again which means they become terminally differentiated and they no longer divide (Al-Shanti and Stewart, 2008). Cyclin-dependent kinase 4 and 6 (Cdk) are essential for the control of proliferation of myoblasts, and their inhibition enhances differentiation of muscle cells (Saab, 2006; De Santa et al., 2007). *Retinoblastoma* protein (pRb) comprises a cell cycle control protein concerned with control of myoblasts propagation and differentiation (Besson et al., 2008), as hypophosphorylated pRb seizes and binds to E2F transcription factors, thereby stopping the transcription of genes necessary for G1/S transition (Ren, 2002; De Falco and De Luca, 2006). Orderly expression of the primary and secondary transcription elements is required by myogenesis (MyoD and Myf5, and myogenin and MRF-4 respectively), bringing about the morphological differences as muscle-specific gene expression (summarised in figure 2) (Le Grand and Rudnicki, 2007). Skeletal muscle makes up most of the body mass, thus disturbed development of fetal muscle causes reduced birth weight and reduces metabolism of fatty acids and glucose in the entire body (Lowell, 2005; Oak et al., 2006). This is why the possible mechanisms of the effect of extracellular elements related to diabetes and obesity on muscle development are given significant attention.

Regulation of the cell cycle

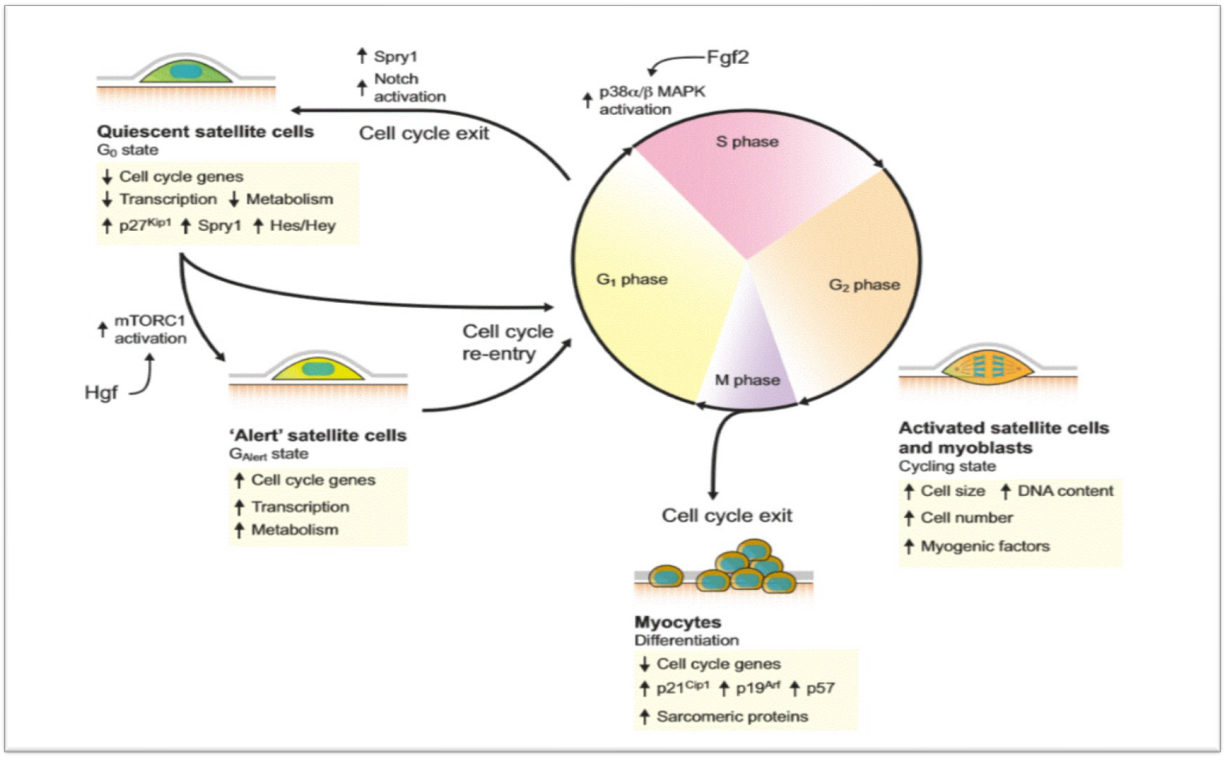

Figure 2: Regulation of the cell cycle.

When conditions permit satellite cells to be dormant, the cell cycle inner controllers keep the satellite cells in a state where they are both dormant and reversible within a G0 state. Once they are activated, the satellite cells make their way back into the cell cycle, either directly or through an intermediary state referred to as the G Alert. Once activated, these cells are able to leave the cell cycle and go back to their dormant state through increased Notch signalling or up-regulating Spry1. These multiplying myoblasts also leave the cell cycle to separate into myocytes and then develop into the myogenic lineage (Dumont et al., 2015).

1.2 The impacts of diabetes on skeletal muscle

Skeletal muscle coordinates body movement by producing contractile forces. They regulate the body's overall metabolism by storing up to 80% of total glycogen and aiding in insulin uptake and amino acid catabolism (Jensen et al., 2011). The prolonged and continuous functioning of skeletal muscle fibres and their consequent exposure to various physical and biochemical factors causes substantial muscle damage (Shadrach and Wagers, 2011). In a healthy individual 70-80 % of consumed glucose is taken by skeletal muscles facilitated by an insulin dependent mechanism (Deshmukh, 2016). Type 2 diabetes mellitus (T2DM) is a metabolic disease which results in raised levels of glucose within the bloodstream or hyperglycaemia, and the absence of glucose within tissues (Shadrach and Wagers, 2011). Diabetes mellitus noticeably reduces the myogenic functionality of satellite cells within skeletal muscle (Abdul-Ghani and DeFronzo, 2010). Different

mechanisms which can cause damage to the health of skeletal muscle have been suggested. These include chronic low-grade inflammation profile (CLIP), impaired extracellular matrix modelling, and oxidative stress (Illustrated in figure 3) (D'Souza et al., 2013). In T2DM, this mechanism is impaired due to insulin resistance (Abdul-Ghani and DeFronzo, 2010). Moreover, it disturbs muscle metabolism causing reduction in intermyofibrillar mitochondrial content and function as well as increase in abnormal lipid deposition. Furthermore, this disturbs switching between fat and carbohydrate oxidation in response to insulin. These changes make the muscle metabolically inflexible, which has impacts on the maintenance of an active and healthy life style (Kelley and Mandarino, 2000).

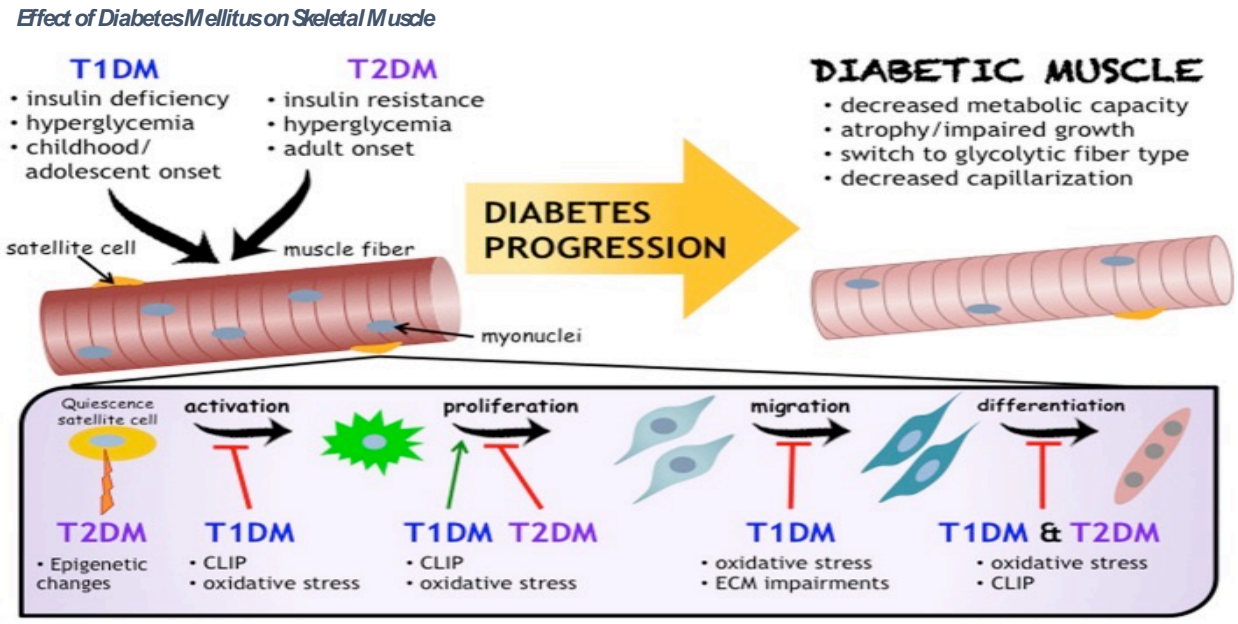

Figure 3: Impact of Diabetes Mellitus on Skeletal Muscle Health .

Chronic low-grade inflammation (also known as CLIP, or chronic low-grade inflammatory profile), oxidative stress, and impaired extracellular matrix remodelling are the common mechanisms that causes skeletal muscle impairment and decreases satellite cell functionality in diabetes mellitus (D'Souza et al., 2013).

A common, often overlooked complication of T2DM is the reduction of healthy skeletal muscle mass and function; this is referred to as diabetic myopathy (D'Souza et al., 2013). Furthermore, Hyperglycaemia can lead to neural damage and alter neuromuscular transmission causing muscle atrophy and weakness in diabetic individuals, this complication known as diabetic neuropathy (could be sensory or motor neuropathy) (Callaghan et al., 2012). In fact, several

factors can lead to muscle and neural wasting in T2DM such as hyperglycaemia, hyperinsulinemia, and hormonal changes like glucocorticoids (Schakman et al., 2008).

1.3 Diabetic myopathy and neuropathy

Individuals with diabetic myopathy normally suffer from alternative extended-term symptoms of diabetes, including peripheral vascular disease, cardiovascular diseases as well as neuropathy (Delaney-Sathy et al., 2000; Ahmad et al., 2014). The connection between skeletal muscle and motor neurons is called the neuromuscular junction (NMJ) which is crucial link in human motor system controlling voluntary muscular movement (Gonzalez-Freire et al., 2014). Muscle denervation, re-innervation or impaired NMJ dramatically alter muscle physiology (Cadot et al., 2015). The operational and morphological alterations of NMJ in diabetes are related to muscle inferiority (Diabetic myopathy) as well as neural impairment (Diabetic neuropathy) (summarised in figure 4). Differences of NMJ transmission would aid in the advancing weakness of flexor and extensor muscles within diabetes (Andersen, 2009).

The structural elucidation of a neuromuscular junction (NMJ)

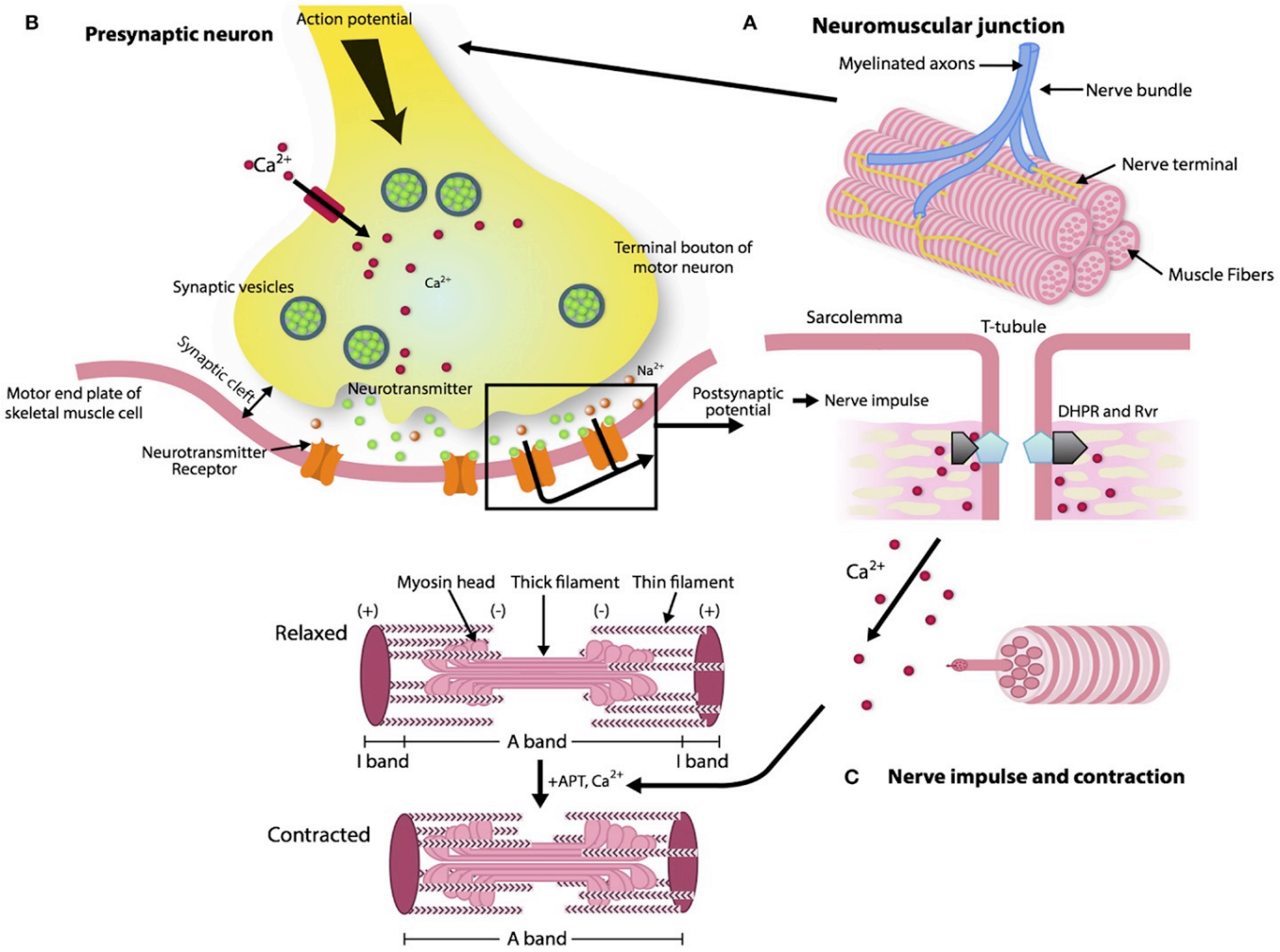

Figure 4: The structural elucidation of a neuromuscular junction (NMJ).

(A, B) The NMJ comprise of three elements: pre-synaptic (motor nerve terminal), intrasynaptic (synaptic basal lamina), and post-synaptic component (muscle fiber and muscle membrane) .When the action potential reaches the motor nerve terminal ,voltage gated calcium channels opens and the calcium flushes inside the neuron from pre-synaptic cleft triggering release of ACh into the synaptic cleft via diffusion. (C) Released ACh binds to AChR present in the Motor end plate of skeletal muscle cell cause activation of (i) the voltage-gated L-type calcium channels(DHPR) located in the surface of sarcolemma and transverse tubules of myofibrils (ii) sarcoplasmic reticulum(SR) calcium release channel ryanodine receptors (RyRs). Calcium released from the sarcoplasmic reticulum through the RyRs binds to troponin C and allows cross-bridge cycling and force production .The structural modifications of these membrane receptors and trans-membrane proteins hindering their functionality are linked to complications observed during diabetic myopathy and neuropathy (Gonzalez-Freire et al., 2014).

The specific mechanisms underlying the advancement of diabetic peripheral neuropathy (DPN) are not totally understood. Nonetheless, DPN is probably the result of diabetes-associated vascular or metabolic disruptions which are not mutually exclusive and could be associated or synergistic (Zochodne, 2007). Such mechanisms result in axonal loss by means of a dying-back, or retrograde deprivation, in addition to peripheral nerve demyelination (Zochodne, 2007). In fact, diabetes mellitus results in long-term impairment and malfunction of different tissues (Calcutt et al., 2009). Specifically, neural impairment caused by diabetes (sensory as well as motor nerve) comprises a major type of neuropathy (Andersen, 2009). Moreover, mitochondrial dysfunction associated with oxidative stress resulting from hyperglycemia or hyperlipidemia are theorised to have a significant impact in DPN (Figure 6) (Picard et al., 2013).

T2DM comprises a common reason for motor neuropathy (motor nerve impairment) resulting in weakness and atrophy of muscles (Andersen, 2009). This complication is accountable for a lack of muscle strength, related to wasting of the distal sections of the lower body, due to denervation resulting from the loss of motor axons and inadequate re-innervation (Ramji et al., 2007). The capability of the body to synchronise motion may be influenced by motor neuropathy, particularly during walking. The foot problem known as Charcot foot may progress due to walking while suffering from motor neuropathy (Said, 2007). Thus, individuals with diabetes are more inclined to encounter greater loss of muscle mass, strength and eminence with time, in contrast to those not suffering from diabetes (Kalyani et al., 2010). The most widespread type of diabetic neuropathy comprises a length-dependent symmetrical neuropathy with major involvement of sensory fibres (Said, 2007) and motor fibers in the sever forms (Dyck et al., 2011). These influences of diabetes on muscle could clarify why individuals with diabetes are in greater risk of developing functional impairment and movement restrictions (Kalyani et al., 2014). Furthermore, the cause for this degeneration of muscle function in individuals with diabetes is yet not clear.

Within humans, loss of motor axon or motor unit (MU) (Illustrated in figure 5) has been measured employing the extensor digotorum brevis (EDB) (Power et al., 2010; Wang et al., 2014). However, within intrinsic foot muscles such as the EDB it can be a challenge to distinguish axonal loss

resulting from physical trauma as opposed to impairment resulting from biochemical factors related to diabetes (Wang et al., 2014). Additionally, assessment of MU loss within muscles with greater function (e.g. tibialis anterior) permits the evaluation of alternative related physiological and clinical features including fatiguability and strength (Wilson and Wright, 2014). It is believed that hyperglycaemia, which is an initial indication in the advancement of diabetes, impairs nerves and causes muscle impairment and the reduction of mass and strength (Gumy et al., 2008). Notably, weakness and muscular wastage related to T2DM could be partly caused by motor unit as well as motor axon loss (Allen et al., 2016).

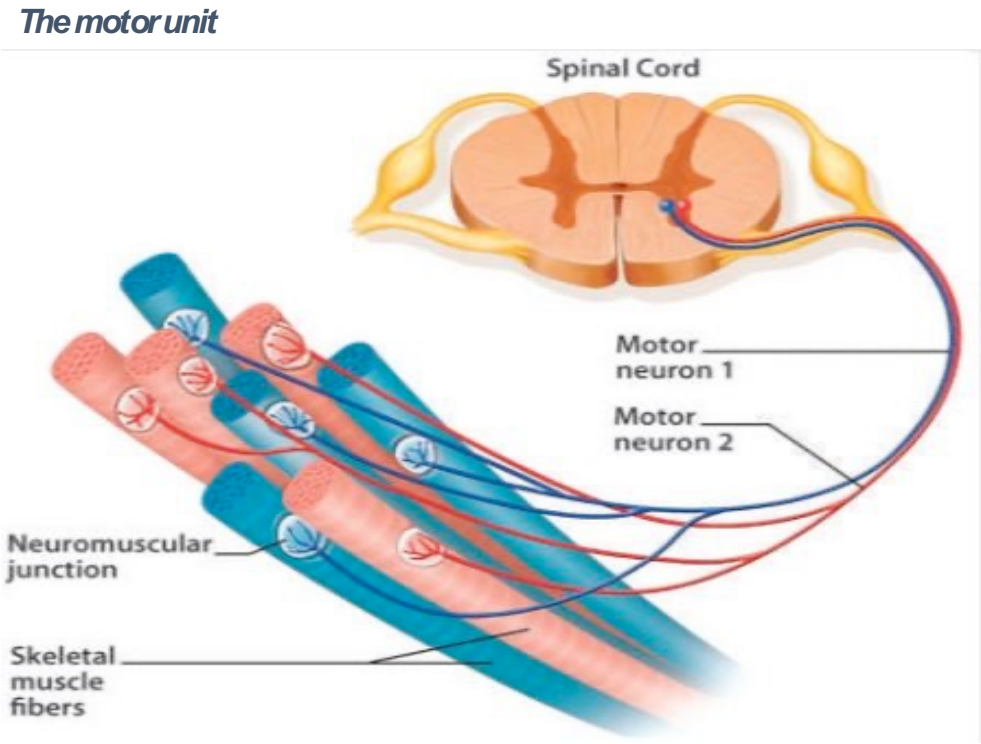

Figure 5: The motor unit

The motor unit consist of muscle, motor nerve and neuromuscular junction. The figure illustrate two individual motor units. The α-motor neuron bodies of the cells are positioned in the spinal cord's ventral horn. Neuron axons leave the ventral horn and enter the synapse and periphery with their corresponding muscle fibers. Every motor unit is made up of a separate α -motor neuron as well as the different muscle fibres innervated by it (Tiryaki and Horak, 2014).

1.4 The Effect of AGEs in inducing diabetic myopathy and neuropathy

Advanced glycation end-products (AGEs) are a broad group of compounds formed by means of a non-enzymatic glycation procedure referred to as the Maillard reaction, have a high impact on the aetiology of diabetic complications (Chiu et al., 2015). Raised absorption of glucose by skeletal muscles is directly proportional to the glucose removal from the body. However, hyperglycemia results in the glycation of enzymes and proteins essential for different cellular activity (Ashraf et al., 2014; Ashraf et al., 2015). Additionally, the endogenous metabolites, methylglyoxal (MG), glyoxal, as well as 3-deoxyglucosone (3-DG) are reactive glycating agents produced through auto-oxidation of glucose which further converts sugars to AGEs (Ashraf et al., 2016; Beisswenger et al., 2005). Non-enzymatic glycation begins with the formation of Schiff bases that are further changed into amadori products and subsequently AGEs (Ahmed and Thornalley, 2007), and the gradual build-up of AGEs within organs and muscle enhances the formation of reactive oxygen species (ROS) resulting in oxidative stress, which is mostly caused by NF-κB signalling pathway leading to mitochondrial dysfunction (summarised in figure 6) (Vlassara and Palace, 2002; de M. Bandeira et al., 2013).

Mechanisms of diabetic neuropathy

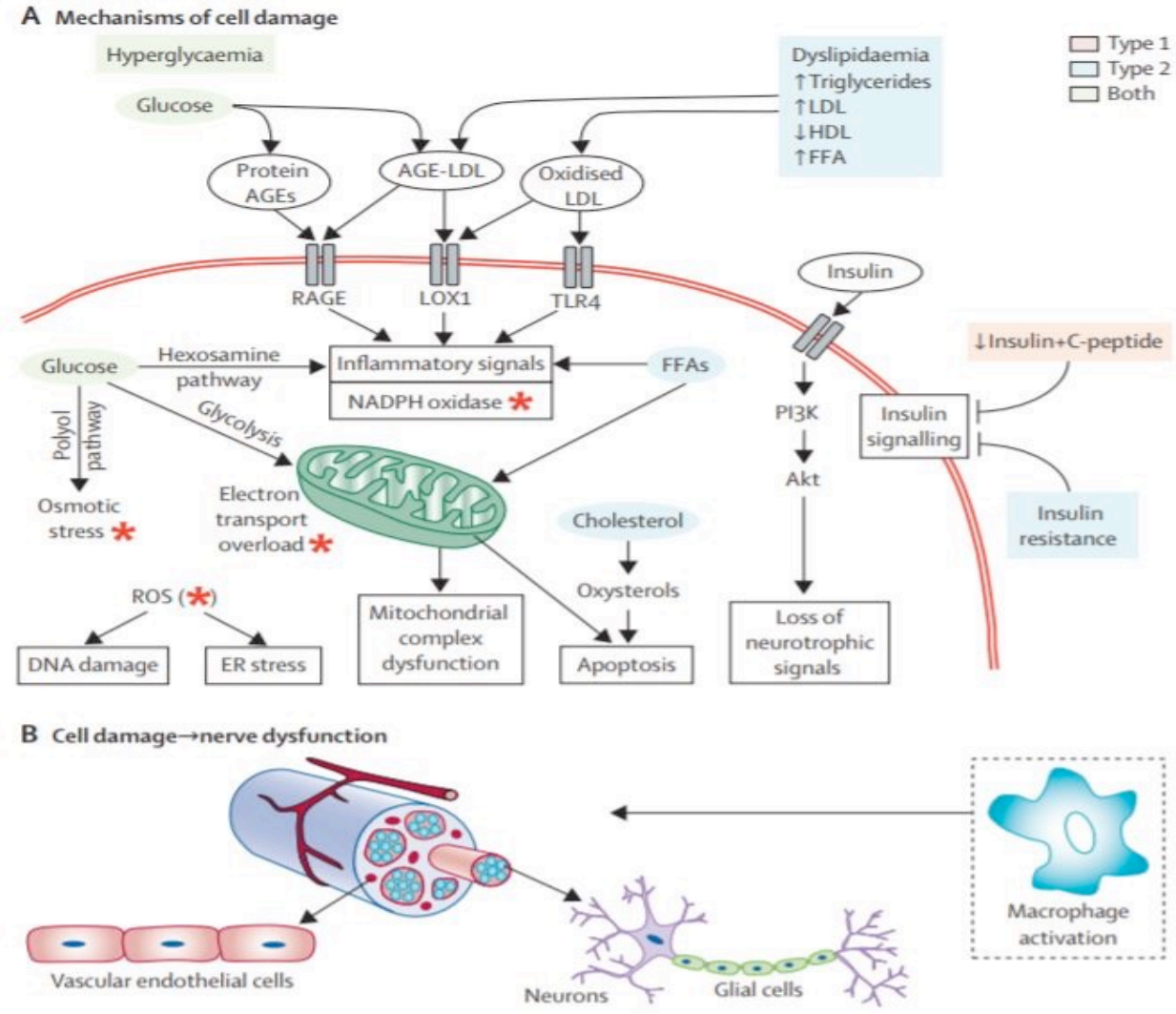

Figure 6: Mechanisms of diabetic neuropathy.

Many factors like apoptosis, endoplasmic reticulum stress, DNA damage, and loss of neurotrophic signaling can cause mitochondrial dysfunction which are related to the pathology of type 1 diabetes , type 2 diabetes or both (Callaghan et al., 2012).

(A) Neuropathy and nerve impairment can be caused by cell damage within neurons, glial cells, and vascular endothelial cells triggering macrophage activation. (B) Mitochondrial dysfunction caused by cell damage play a significant role in the complications of diabetes mellitus including nerve dysfunction and diabetic neuropathy.

AGE=advanced glycation end products. LDL=low-density lipoprotein. HDL=high-density lipoprotein. FFA=free fatty acids. ROS=reactive oxygen species (red star). ER=endoplasmic reticulum. PI3K=phosphatidylinositol-3-kinase. LOX1=oxidised LDL receptor 1. RAGE=receptor for advanced glycation end products. TLR4=toll-like receptor 4.

AGE-modified proteins bind to RAGE (AGE- receptors on cell exterior) and raised expression of RAGE has been documented on the endothelial cells, cardiac myocytes and skeletal muscle cells in individuals with diabetes (Ramasamy et al., 2005). Additionally, contact amid RAGE and AGEs have been documented to stimulate intracellular signalling, prompt expression by genes, generate free radicals as well as pro-inflammatory cytokines, therefore, this interaction has been proposed to have a significant part in the development and advancement of diabetes (Kim et al., 2005). The amassment of AGE takes place or enabled under oxidative stress (Snow et al., 2007). Overall, the AGEs build up is particular to tissue, changes the structural features of proteins, as well as decreasing their tendency to breakdown (Singh et al., 2014). Apart from their function within the pathogenesis of diabetic complications, current studies additionally portrayed that AGEs could damage insulin activity by means of various cellular pathways: they intrude in the intricate insulin pathway, alter the insulin molecule as well as reduce release of insulin (Cassese et al., 2008). The skeletal muscle cells make up the majority of the insulin stimulated glucose utilisation (Uribarri et al., 2011). As a result, some studies proposed that the myofibrillar protein glycosylation comprises a feasible mechanism supporting the reduction in muscle functioning associated with age, have noted the build-up of AGEs within the skeletal muscles of ageing rats (Ramamurthy and Larsson, 2013). Furthermore, several studies have stated that AGEs deposits within the myofibres of the extensor digitorum longus of ageing rats (Snow et al., 2007) as well as the soleus muscles of rats with diabetes (Snow and Thompson, 2009). Aggregation of AGEs within the skeletal muscles has additionally been observed within ageing human subjects, accompanied by reduced muscle strength (Dalal et al., 2009). A further research established that mice with streptozotocin-induced diabetes with extensive accumulation of AGEs in muscles of rear limbs displayed a larger reduction in muscular mass, endurance of muscles as well as regenerative ability, inferring that AGEs have an important connection with the damage in mass and force of muscles, which corresponded with the results from prior researches (Chiu et al., 2016).

Researches with diabetic rodents have reported that myelin structure in the central as well as peripheral nerve system experience nonenzymatic glycation (Ramasamy et al., 2005). It has been

proposed that AGE-altered peripheral nerve myelin is vulnerable to phagocytosis from macrophages, and this prompts macrophages to release protease, which could assist in demyelination within diabetic neuropathy (Sango et al., 2017). Main axonal cytoskeletal proteins including tubulin, actin in addition to neurofilament are subjected to glycation as well. Such axonal proteins are essential for the sustenance of axonal functioning and arrangement, and their alteration through glycation could change the structural as well as operational axon features, thus aiding wastage and degradation of the axon, in addition to the reduction of axonal signalling (Sugimoto, Yasujima and Yagihashi, 2008). However, researches investigating the influence of AGEs on the operation of skeletal muscle within diabetic animals as well as humans remain few (Semba, Nicklett and Ferrucci, 2010; Sugimoto, Yasujima and Yagihashi, 2008).

1.5 *In vitro* model of human immortalised skeletal myoblasts, motor neurons and neuromuscular junctions (NMJs)

1.5.1 *Challenges of current animal and humans-based models*

The greater majority of fundamental scientific studies on T2DM have been carried out within animal models, for species varying between fruit flies and primates, and most commonly rodents species (Furman, 2015). Years of studies on animals have brought about a greater knowledge and understanding underlying mechanisms of glucose regulation, and differences in natural history particular to species, clinical indications, complications, and medication reactions in the animal models (King, 2012). Nevertheless, such species variations avert the recurrence of human T2DM within animal models, and thereby disturb the dependable conversion of therapeutic and mechanistic conclusion for clinical gain (Zeeshan, Chandrasekera and Pippin, 2018). Several drugs are being applied clinically of differing efficiency and strength, for treatment or precaution against T2DM. Yet, the majority have minor or no influence on disease advancement, neither do they comprise cures for T2DM, and they do not obviously extend life expectancy (King, 2012; Chandrasekera, 2014). Due to species-species variations at each step of glucose regulation, concerns regarding the conveyance of results based on animals to human T2DM, and identification of the requirement for an additionally human-particular study are increasing (Chandrasekera, 2014). Provided that the research on disease mechanisms is a chief concern, and that the present animal-based study is not dependable for human implications (Furman, 2015). Likewise, the complex nature of the culture system contributing to the inconsistent experimental reproducibility is the primary drawback of nerve muscle cocultures with mouse, rat, primary human myoblast, and induced pluripotent stem cells (hiPSCs) (Demestre et al., 2015; Umbach et al., 2012; Harper et al., 2004; Guo et al., 2014; A.-S. Arnold et al., 2012). Out of many, the variable serum composition can be accounted for the irregularity observed in reproducibility and have high incidence on experimental treatments within the system (Guo et al., 2014). Furthermore, some studies have established link between the serum composition and slow myelination of motor neurons *in vitro* (Rumsey et al., 2009). Another key points the limited proliferative capacity, poor cell purity and high degree of cellular senescence throughout cell expansion are the main drawback of coculture models developed using primary human skeletal muscle stem

cells (i.e. primary myoblasts) acquired from muscle biopsy (Mouly et al., 2005). The developments in the application to generate myoblasts from human embryonic stem cells (hESC) (Stockmann et al., 2013) can be used to rectify the above-mentioned setbacks. Thus, the complex, multifactorial aetiology of T2DM could be recapitulated in patient-specific and disease- specific human induced pluripotent stem cells (Jang et al., 2012). These cells are an invaluable platform for disease modelling, high-throughput drug discovery screening, preclinical toxicity assessment, and personalized medicine development relevant for specific manifestations of T2DM (Kawser Hossain et al., 2016). A plethora of human mimetic models can be developed from patient-specific cells at different clinical stages, and the cells can even be subjected to ageing techniques *in vitro* (Chun et al., 2010). It is crucial to use human stem cells rather than rodent stem cells, since species-specific molecular signatures, cellular signalling, growth rate, surface markers, developmental potential, satellite cell activation, and a host of other factors, will prevent accurate data extrapolation from rodents to humans (Zeeshan, Chandrasekera and Pippin, 2018). In addition to the types of cells used, it is important to employ physiologically relevant cell culture conditions, to closely simulate *in vivo* human glucose physiology (Chandrasekera, 2014). Furthermore, typical *in vitro* models of neuromuscular disease are generally established using animal derived cells (Haase, 2006; Prather et al., 2013) and/or the use of skeletal muscle cell monolayer cultures, which lack the functional innervation, and hence NMJs, so important for muscle differentiation (Suuronen et al., 2004). Up to the present, all animal models which have been studied are inappropriate for scrutiny of diabetic myopathy and neuropathy as a result of their major drawbacks and weaknesses. A few numbers of researches have investigated the effect of diabetic myopathy and neuropathy in depth using *in vitro* human models.

1.5.2 Development of in vitro novel human-based model

To our knowledge no researches have studied the effect of diabetic myopathy and neuropathy towards NMJ modelling as well as muscle function, solely employing human coculture model. Thus, this study aims to comprise an ongoing endeavour for the creation of novel model which have a key and significant place within diabetes investigation research. With this intention, this project investigates the influence of various concentrations of glucose and AGEs on skeletal muscle, particularly the influence towards myogenic morphology and differentiation, through

establishing a functional *in vitro* human model. A significant element of this project the use of immortalised human skeletal muscle myoblasts (HSMM) , which are solely accessible to research laboratories within the UK (generously made available by Professor Browne, Paris) (Mamchaoui et al., 2011). Initially in this study HSMM monoculture model was treated with (5-15 mM/ml) D-glucose (L-glucose and mannitol were used for control) and (50-200 µg/ml) of AGEs (BSA used for control). Furthermore, a complex coculture model established by Dr.Al-Shanti's group which mimics *in vivo* human NMJ platform will be used . This model employs HSMM and hESCs -derived neural progenitor cells (NPCs) which progress into motor neurons within muscle differentiation media in the absence of any neural growth factors or serum (shown in Figure 7). As far as we know, this is the initial research to be performed employing only wholly pertinent NMJs human model to study diabetic myopathy and neuropathy. Thus, this platform has considerable potential for advancement of clinically pertinent *in vitro* models of neuromuscular disease.

Human Neuromuscular Junction model

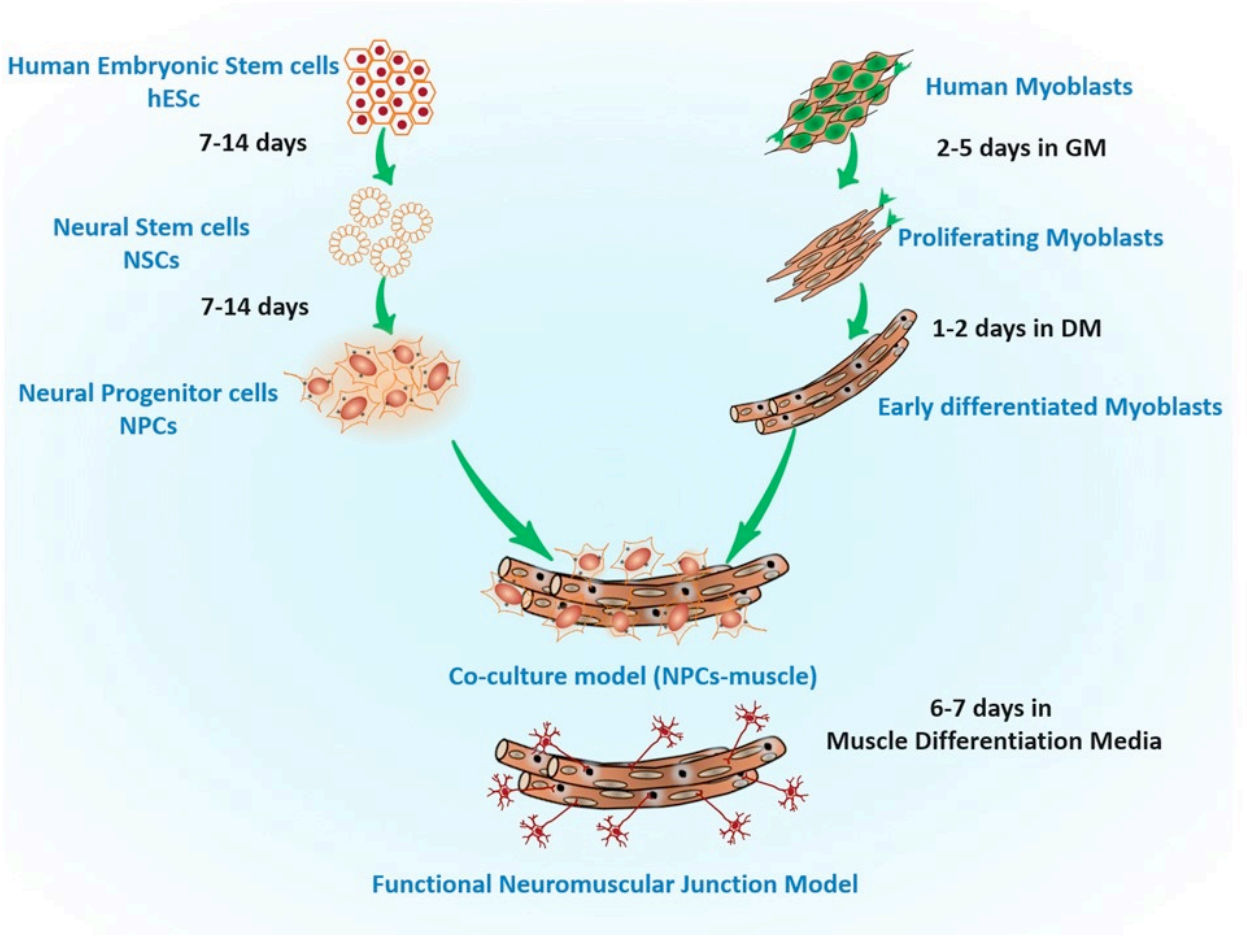

Figure 7: Functional human Neuromuscular Junction model (NMJ).

Human immortalised myoblasts were co-cultured with hESCs-derived human neural progenitor cells (NPCs). Over the course of 7 days within muscle differentiation media in the absence of any neural growth factors or serum, myoblasts differentiated into myotubes and NPCs differentiated into motor neurons that branched to form multiple NMJ innervation sites along myotubes (Used with permission from Dr. Al Shanti's group)

1.6 Aims and objectives

Myopathy and neuropathy in diabetes are associated with reduced muscle force, which portrays inferior movement and physical operation, ultimately influencing the regular physical lifestyle of the diabetic patient. Thus, this project aims to assess various levels of glucose and AGEs on skeletal muscles myotubes (monoculture) to gain an insight into the mechanisms involved in diabetic myopathy. Additionally, employing novel functional human NMJ model, applying human immortalised myoblasts as well as hESCs- NPCs established by Dr. Al Shanti's group, we intend to study the mechanisms of NMJ development and degradation subject to induced *in vivo* human diabetic neuropathy.

The main objectives are:

- *Culture human myoblast cell to develop a viable and functional human model using HSMMs (monoculture):*
  - Cell culture will be treated with various concentrations of D-glucose (5-15mM/ml), L-glucose and mannitol will be applied as control.
  - To determine the significances of various concentrations of glucose concerning nuclear positioning and growth, myogenic differentiation and morphological alterations.
  - Treatment of cell culture with varying concentrations of AGE (50-200 µg/ml).
  - Determine the effect of various concentrations of AGE towards myogenic growth and differentiation.

- *Mimic the diabetic environment in humans, nerve-muscle cocultures treatment with different concentrations of AGEs (50-200 µg/ml).*
  - To determine the effect of varying AGE concentrations on coculture morphological alterations, myogenic differentiation, growth and nuclear position.
  - AGEs influence on motor neuron differentiation (axonal length).
  - Nerve formation.
  - NMJ innervation.

- *Estimate mitochondrial respiration through quantifying the oxygen consumption rate (OCR) of cells in monoculture and coculture using the Seahorse XFp analyser:*

  - To investigate metabolic dysfunction within diabetic myopathy and neuropathy which is related to changes in mitochondrial respiration activity and morphology (mitochondrial dysfunction).

1.7 Purposes and Hypotheses

Overall, the purpose of this research project is to investigate the potential involvement of high glucose and AGEs effects on myogenic differentiation and morphology of skeletal muscles and nerve cells by developing a novel functional human model. Therefore, this project's hypotheses are as follows:

- It is hypothesised that skeletal muscle myoblasts (monoculture) when treated with high levels of glucose and AGEs will have detrimental effects on myogenic differentiation (myotubes formation) and nuclear positioning and growth.

- It is hypothesised that the nerve-muscle cocultures when treated with high concentrations of AGEs will interfere with the nerve-muscle morphology and myogenic differentiation, as well as nuclear positioning of skeletal muscles, and its effect on motor neuron differentiation (axonal length).

- It is hypothesised that AGE causes interfere with mitochondrial respiration within skeletal muscle myoblasts (monoculture) and nerve-muscle cocultures which could be related to mitochondrial dysfunction.

2. Methods and Materials

2.1 Immortalised human skeletal muscle cell culture

The partners we collaborate with at the Institute of Myology, which is based in Paris, donated to us a non-commercial 25 years old (C25) immortalised human skeletal muscle cell (SkMC) line (Mamchaoui et al., 2011). A vial, which was frozen and contains 1ml of $1x10^6$ cells each suspended in 10% dimethyl sulfoxide and 90% fetal bovine serum was thawed before being moved into a 9 ml conical tube with a prepared growth media (GM) that will facilitate the proliferation of SkMC (Table 1).

Table 1: Growth media for SkMC Proliferation.

Growth media components	Concentration
Dulbecco's Modified Eagles Media (DMEM) from Lonza (Nottingham, UK)	60% (v/v)
Medium 199 with Earle's BSS from Lonza (Nottingham, UK)	20% (v/v)
Heat inactivated fetal bovine serum (FBS) from Gibo (Loughborough, UK)	20% (v/v)
L-glutamine from Lonza (Nottingham, UK)	1% (v/v)
Fetuin from fetal bovine serum from Sigma-Aldrich (Dorset, UK)	25µg/ml
Recombinant human fibroblast growth factor-basic (FGFb) from Gibco (Loughborough, UK)	0.5ng/ml
Recombinant human epidermal growth factor (EGF) from Gibco (Loughborough, UK)	5ng/ml
Recombinant human hepatocyte growth factor (HGF) from Sino Biological Inc. (Suffolk, UK)	2.5ng/ml
Recombinant human insulin from Sigma-Aldrich (Dorset, UK)	5µg/ml
Dexamethasonne from Sigma-Aldrich (Dorset, UK)	0.2µg/ml
Penicillin/Streptomycin (Sigma, UK)	1% (v/v)

2.2 Monoculture model

2.2.1 Proliferation

The 10 ml C25 suspension was moved into T75 flasks. Using a 5% CO_2 atmosphere at a temperature of 37°C the flasks where incubated. This was done to the level where the cell density was at 80% confluence. ImageJ software was used for quantifying confluency (Schneider et al., 2012) by calculating the total myoblast area (MA); calculated by counting the total area of myoblasts in a field over the entire image x 100 (Ren et al., 2008; Ricotti et al., 2011). For assessment, five fields of view at 10x magnification were chosen at random. Once the confluent of the flasks reached 80%, GM was removed from the flasks. This was followed by washing, twice,

of the cells using Dulbecco's Phosphate Buffered Saline (DPBS) from Lonza (Nottingham, UK). Then with 2 ml of TrypLE™ Express Enzyme from Gibco (Loughborough, UK) the cells were disassociated and incubated at 37°C in 5% CO_2 for 5 minutes. The 2 ml disassociated cell suspension then was transferred into a conical tube and homogenized with 8 ml of GM. Using a 20 µl of Trypan Blue Stain (0.4%) obtained from Lonza (Nottingham, UK), and 20 µl of cell suspension, the cells were counted. The formula used for calculation of viable cells/ml was as follows: [Average number of live cells in one large corner square x dilution factor x 10^4].

2.2.2 Differentiation

Using a concentration of $1.5x10^5$ cell/ml in GM in 6-well plates pre-coated with a 0.5% gelatine solution, the C25 SkMC were seeded. In a 5% CO_2 atmosphere at temperature of 37°C, the cells were incubated for a period of 24 hours. Following this, GM was removed, and the cells were washed, using DPBS, two times. Then differentiation media (DM) (Table 2) was added to each well (2ml) and cells were incubated for a period of 96 hours with a 5% CO_2 atmosphere at a temperature of 37°C. The assessment of the phenotypic differentiation (alignment, elongation and fusion) was achieved with the use of phase contrast microscopy.

Table 2: Differentiation media components

Differentiation media components	Concentration
Dulbecco's Modified Eagles Media (DMEM) from Lonza (Nottingham, UK)	500 ml
L-glutamine from Lonza (Nottingham, UK)	1% (v/v)
Recombinant human insulin from Sigma-Aldrich (Dorset, UK)	10 µg/ml
Penicillin/Streptomycin (Sigma, UK)	1% (v/v)

2.3 Coculture model

2.3.1 Neural Differentiation of hESCs

Induction of neuroepithelial clusters (NECs)

In mouse embryonic fibroblasts (MEF) growth media, mouse embryonic fibroblasts (MEF, Cell Biolabs, UK) were cultured and passaged using a ratio of 1:4. Using 0.1 µg/ml Mitomycin C (Sigma,), MEFs were inactivated mitotically at passage 4. the UK StemCell Bank, under the project SCSC10-48, supplied the Shef3 Human embryonic stem cell (hESC) line which was kept on mitotically inactivated mouse embryonic fibroblasts (MEFs) in hESC medium (Table 3) in 96- well-plates. Every 5–7 days, the hESCs were passaged mechanically before being conditioned to feeder-free culture by TrypLE Express enzyme dissociation and plated at high density (1:1) onto hESC-qualified MatrigelR (Corning) coated flasks in mTESR (STEMCELL Technologies). Using TrypLE feeder-free hESCs were dissociated, for neural induction, and then they were re-plated in neural induction 14 medium (NIM,Table 4) in uncoated, V-shaped 96-well plates at a density of $1x10^4$ cells/well. Neuroepithelial clusters (NECs) formed within 24 hours.

Table 3: Human embryonic stem cell (hESC) media for cells on MEFs.

hES/MEF cell medium components	Volume
Dulbecco's Modified Eagles Media (DMEM)- F12 (1:1) from Lonza (Nottingham, UK)	38.5 ml
MEM Non-essential amino acids (NEAA) (Life Technologies, UK)	0.5ml (1x)
bFGF (R&D systems, UK) (100ug/ml)	5uL (10ng/ml)
Penicillin/Streptomycin (Sigma, UK)	0.5 ml (1x)
Knockout Serum Replacement (KSR) (Gibco, Life Thechnologies, UK)	10ml (20%)

Table 4: Neural Induction Medium (NIM)

NIM components	Volume
Dulbecco's Modified Eagles Media (DMEM)- F12 (1:1) from Lonza (Nottingham, UK)	48.5 ml
MEM Non-essential amino acids (NEAA) (Life Technologies, UK)	0.5ml (1x)
Penicillin/Streptomycin (Sigma, UK)	0.5 ml (1x)
N2 supplement (Life Technologies, UK)	0.5 ml (1x)
Heparin (Sigma, UK) (2mg/ml)	50ul (2µg/ml)
Poly (vinyl alcohol) (PVA) (Sigma, UK)	4mg/ml
bFGF (R&D systems, UK) (100ug/ml)	10uL(20ng/ml)

Generation of neural rosette-forming progenitor stem cells (NRPCs)

On a daily basis, for five days, the medium was replaced. On the sixth day, using 96-well-plates in NIM onto 20 µg/mL laminin (Milipore)-coated dishes, aggregates were re-plated. This was done to permit for the formation of neural rosette (2-3 days).

Expansion of neural progenitor cells

Before being re-plated, using 96-well-plates, onto laminin-coated dishes in neural expansion medium (NIM plus 1x B27 supplement [Life Technologies]), neural rosette clusters were isolated mechanically. Using TrypLE, early-and late passage NPC were cultured in similar settings and passaged 1:3. Using a GEP-reporter lentivirus system, the NPCs were transferred, in order to monitor NPCs differentiation into motor neurons.

2.3.2 Coculture of NPCs and Human myoblasts

In a 5% CO_2 environment, at a temperature of 37°C, in 6-well plates pre-coated with a 0.5% gelatine solution, human myoblasts were incubated for a period of 24 hours. This was then followed by replacing the GM with DM. At concentration 25 x 103/ml, NPCs were present, and they were also incubated in a 5% CO_2 setting at a temperature of 37°C for 7 days (Schematic procedure illustrated in Figure 8).

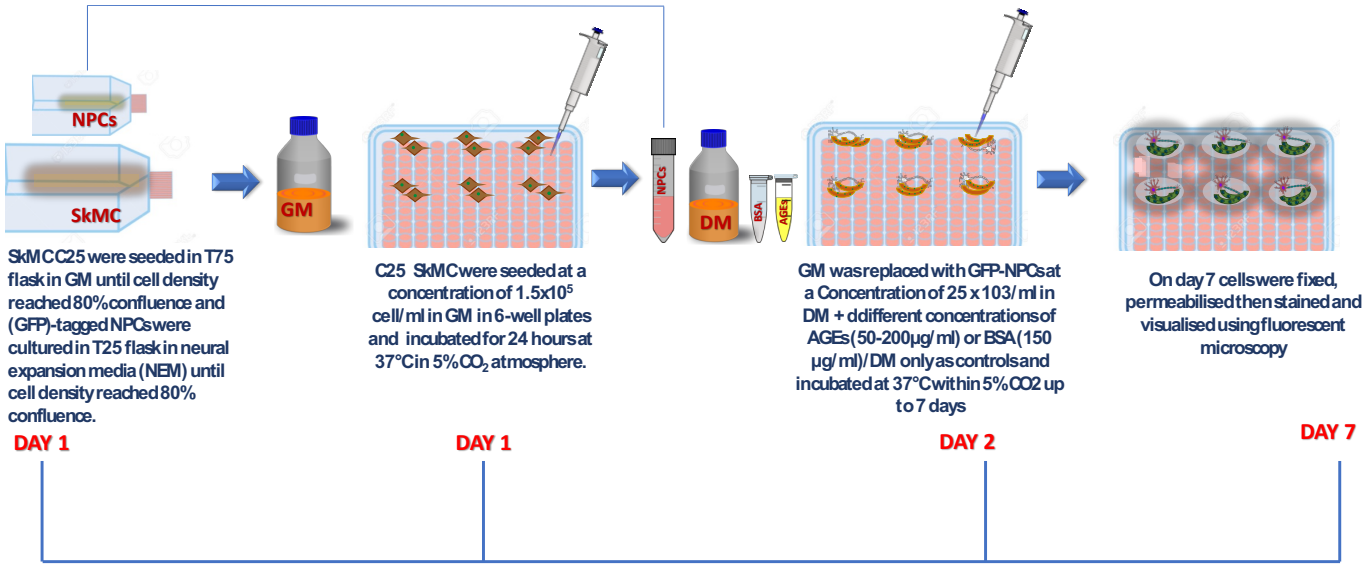

Figure 8: Schematic procedure of nerve- muscle coculture.

2.4 Measurement of axonal growth in coculture(nerve-muscle)

The NPCs with a GFP-reporter lentivirus in the *in vitro* coculture model were imaged under fluorescent microscope (Leica CTR 6000), over the 7 days of culture with different concentrations of AGEs (50-200 µg/ml) treatments or BSA (150 µg/ml) and DM as controls. The axonal length of the differentiating motor neurons was measured over 7 days *in vitro* (DIV) using Image J (procedure illustrate in figure 9), assessed at 20X magnification (at least five random fields of view selected).

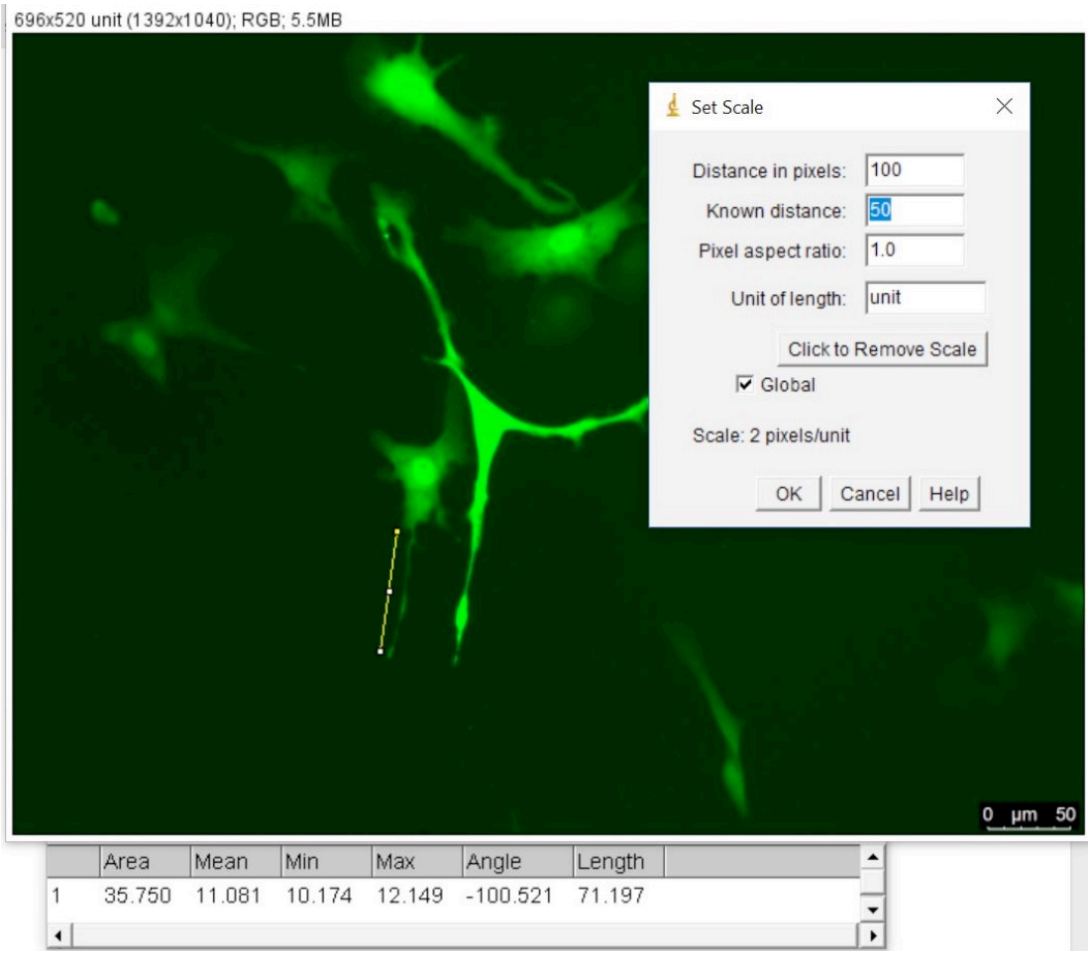

Figure 9 : Axonal length measurement of motor neurons using imageJ software

Images were acquired by using fluorescent microscope (Leica CTR 6000) at 20X magnification of representative five fields of view, selected at random. Then axonal length was measured using imageJ software using the "analyse →tools →ROI manger" function tab and the same procedure were applied to all images. The "analyze particle" function was used to set the scale, with pixel size (pixel^2).

2.5 Myogenic differentiation and differentiated treatment

Various Dextrose glucose (D-glucose) concentrations from Sigma-Aldrich® (Dorset, UK), ranging from 5 to 15 mmol/ml, were added to the monoculture model with DM media (which according to the manufacturer description, contained 4.5g/L (25 mmol/l) glucose). At similar concentrations, mannitol from Sigma-Aldrich® (Dorset, UK) and L-isomer of glucose (L-glucose) from Alfa Aesar® (Lancashire, UK) were used as an osmotic control while the negative control was achieved with DM. On the fourth day in monoculture, the effects of glucose on muscle differentiation was assessed through differentiation parameters which were scored through the analysing diameters, multinucleated myotubes, and cross-sectional areas (Al-Dabbagh et al., 2015). While live cell imaging, immunofluorescent staining, and confocal microscopy were used to determine morphology.

2.6 Advanced glycation end-products (AGEs) Preparations

The model proteins for the glycation experiments were bovine serum albumin (BSA) (10mg/ml). In Methylglyoxal (MG, 0.1 M) in sodium phosphate buffer (0.1 M, pH 7.4, with 0.1% sodium azide to inhibit bacteria) protein was incubated, for three days, at a temperature of 37°C. To get rid of unbound sugars, the glycated BSA was dialysed against distilled water. The dialysis was done by stirring the samples at a temperature of 4 °C. The distilled water was changed daily up to the point when equilibrium was attained. Without MG, non-modified BSA was put through similar preparation conditions. The MG-BSA-AGEs that resulted were defined by fluorescence spectrophotometer (Luminescence spectrometer model LS 30 from Perkin Elmer LAS Ltd., Buckinghamshire, UK). The emissions of the fluorescence spectrophotometer where 420nm after excitation at 350nm. This provided confirmation that the MGBSA-AGEs had higher intensity when compared to non-modified BSA. The detoxi-gel endotoxin-removing gel columns (Thermo Scientific, Rockford, USA) were used to remove bacterial endotoxins from MG-BSA-AGE solutions and non-modified BSA. E-toxate kit, based on the Limulus Amebocyte lysate assay, was used to measure non-modified BSA solutions and MG-BSA-AGEs endotoxin levels. The results indicated that these levels were lower than the detection limit (b0.125 EU/ml). Bradford-based assay (Bio-Rad Laboratories, Hertfordshire, UK), were used to determine concentrations of protein, where BSA was the standard.

Next for one day the SkMC monoculture or cocultures were cultured in six-well plates with GM. They were then changed with DM containing different concentrations of AGEs (50-200 µg/ml) or control groups (BSA (150 µg/ml) or just DM), during the seven days of differentiation for the coculture and four days for monoculture. Then differentiation parameters assessed by analysis of multinucleated myotubes, diameters and cross-sectional areas were used for assessing the AGEs effect (Al-Dabbagh et al., 2015). While live cell imaging, immunofluorescent staining, and confocal microscopy were used to determine morphology.

2.7 Immunocytochemistry and Differentiation parameters

Using 4% paraformaldehyde, cells were then fixed before being incubated at a temperature of 21°C for eight minutes. This was then followed by a washing of cells three times using DPBS and then permeabilised with perm/wash buffer from BD Biosciences (Oxford, UK). For a period of 30 minutes, they were then incubated at a temperature of 21°C. After removing the Perm/wash buffer, DPBS was used to wash the cell for the last time. This was then followed by a staining of the cells using 5 µg/ml Anti-Myosin Heavy Chain Alexa Fluor® 488 from eBioscience (Hatfield, UK), 5 units/ml Texas Red®-X Phalloidin from Invitrogen (Paisley, UK), and 2 ng/ml 4',6-Diamidino-2-phenylindole dihydrochloride (DAPI) Sigma-Aldrich® (Dorset, UK). Using the Leica DMI6000 B inverted microscope from Leica Microsystems (Milton Keynes, UK), the stained cells were visualised for fluorescent microscopy. Differentiation parameters were measured using ImageJ (Table 5). At 20X magnification, five fields of view, selected at random were assessed.

Table 5: Differentiation parameters (Ren et al., 2008; Ricotti et al., 2011; Grubisic et al., 2014).

Differentiation parameters	Formula
Aspect ratio (AR)	(myotube length)/ (myotube width)
Fusion index (FI)	[(total number of nuclei per myotubes)/(total number of nuclei in field)] (100)
Myotube area (MA)	[(total area of myotubes in a field)/ Total area of the field)] (100)

2.8 Determination of oxygen consumption

A Seahorse Bioscience XFp analyser (Agilent, Santa Clara, CA, USA), was used for measuring the skeletal muscle's mitochondrial bioenergetics. This is a tool that has the capacity to measure the

amount of oxygen consumed by mitochondria in live cells. The oxygen consumption rate (OCR) was determined by the Agilent Seahorse XFp analyser.

C25 SkMC (monoculture) and Nerve-muscle cells (cocultures) were seeded in XFp Miniplate. The seeding was done at a density of 7000 cells/well in 100 µl in GM. They were then incubated, for 24 hours, at a temperature of 37 °C under conditions of 5% CO_2. This was followed by changing with DM with varying concentrations of BSA (150 µg/ml), AGEs (50-200 µg/ml) or DM only, for a period of seven days of differentiation for the coculture and four days for the monoculture. In the coculture, at a density of 2500 cells/well, NPCs were seeded with DM.

One day before the assay, in XF Calibrant, XFp Sensor Cartridge was hydrated in a non- CO_2 at a temperature of 37 °C overnight. On the day of the assay, after the removal of DM, it was replaced with 180 µL non-buffered assay medium that consisted of Agilent XF Base Medium with added 10 mM glucose, 10 mM pyruvate, and 2 mM glutamine, pH 7.4. Then for an hour, the plate was put into a non-CO_2 incubator at a temperature of 37 °C.

Ahead of the process of measuring rotenon/antimycin A and carbonyl cyanide 4 (trifluoromethoxy) phenylhydrazone (FCCP), and oligomycin were placed into the sensor cartridge injection ports. The resulting concentration of the above-mentioned compounds was 1 µM and after each injection, three measurements were taken. For the Mito Stress Test, the Miniplate was placed into calibrated XFp analyser. With the aim of getting the utmost effects on mitochondrial respiration, Cell Mito Stress Test Kit was pre-optimized in the following manner: 1 µM oligomycin (complex V inhibitor), 4 µM FCCP (a respiratory uncoupler), and 1 µM rotenone/antimycin A (inhibitors of complex I and complex III).

Once the experiment had been completed, the OCR was recorded over time, normalisation was done for cellular protein content/well, and correction was done for any extra consumption of O_2 by mitochondria. The Bradford reagent (Bio-Rad, Hercules, CA) was used to determine the concentration of protein with reference to bovine serum albumin standard curve. Data of OCR were expressed as pmol/min/µg protein. All the experiments were done trice. From the consequent bioenergetics profiles, detailed information can be obtained on the individual elements of the respiratory chain. Ultimately, the number of mitochondrial function parameters that were calculated from the bioenergetics profile was six. These are basal respiration, non-

mitochondrial respiration, ATP production, spare respiration capacity, maximal respiration, and proton leak (Figure 10). After the computation of data, it was automatically displayed by Seahorse XF Mito Stress test report generator. The bioenergetics profiles which resulted were analysed using Wave Desktop 2.3.0 (Seahorse Bioscience, North Billerica, MA, USA)

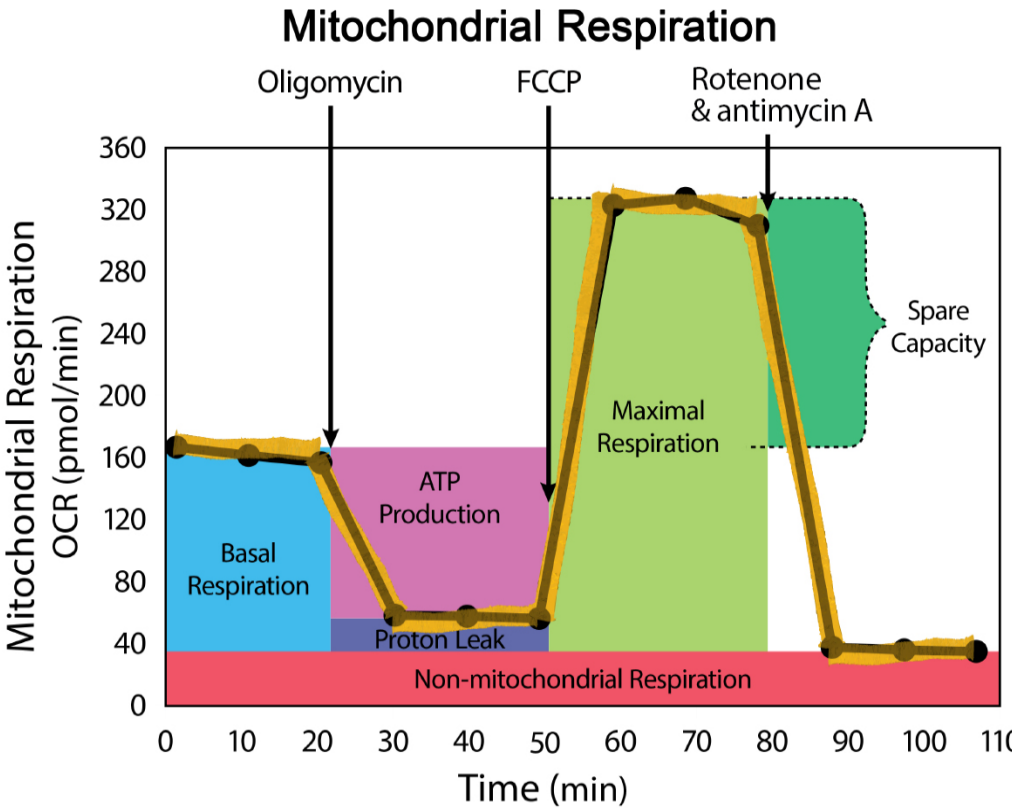

Figure 10: Agilent Seahorse XFp Cell Mito Stress test.

Agilent Seahorse XFp Cell Mito Stress Test profile of the important parameters of mitochondrial respiration. Sequential compound injections measure basal respiration, ATP production, proton leak, maximal respiration, spare respiratory capacity, and nonmitochondrial respiration.In the assay Basal respiration process, the consumption of oxygen employed in meeting the needs of the cells under baseline conditions happened first ahead of the injection of the first compound: Oligomycin (1µM). ATP synthase is blocked by Oligomycin which eventually shows the percentage of oxygen consumed at basal respiration which was used in the production of ATP in order to meet the cell's energy needs. The addition of FCCP (4µM) which has the capacity to prompt the respiratory chain to work at its highest capacity, was used for measuring OCR. Antimycin A (1µM) and Rotenone (1µM) were then added with the result being a blocking of complex I so that Non-mitochondrial respiration could be measured. To measure proton leak, the amount of oxygen not used to couple ATP was used. Extra respiratory capacity was used to measure the ability of cells to meet energy demands (Brand and Nicholls, 2011).

2.9 Statistical analysis

Results were analysed using GraphPad Prism version 7.0 (La Jolla, CA, USA). Statistical analysis for the comparison of more than two means as achieved by one-way ANOVA followed by Tukey's Multiple Comparison Test. Results were expressed as mean ± standard deviation (mean ± SD), with an asterisk (*) indicating statistical significance and it corresponds to (*) $P \leq 0.05$, (**) $P \leq 0.01$, (***) $P \leq 0.001$ and (****) $P \leq 0.0001$. significant results were accepted at ($P < 0.05$).

3. Results:

Outline of results

Initially in this study SkMC monoculture model was treated separately with (5-15mM/ml) D-glucose (L-glucose and mannitol were used as an osmotic control while the negative control was achieved with DM.) and (50-200 µg/ml) of AGEs (BSA used for control). Moreover, the novel NMJ model, applying SkMC and NPCs was treated with different concentrations of AGEs (50-200 µg/ml) and BSA used for control parameters. The effect of varying treatments on mono and coculture morphological alterations, myogenic growth, nuclear position and AGEs influence on motor neuron differentiation (axonal length) were analysed. Furthermore, the effect of AGEs on mitochondrial bioenergetics of both models were measured.

3.1 Monoculture treatment with glucose:

3.1.1 SkMC differentiation parameters:

Differentiation parameters which are standard tool to assess degree of myogenic differentiation like fusion index, myotube area, and aspect ratio were measured using immunofluorescent images generated via DAPI nuclear counterstain and MyHC, to quantify any significance differences in the differentiation of treated SkMC at 96 hours with various concentration of glucose. At similar concentrations, of mannitol and L-glucose were used as an osmotic control while the negative control was achieved with DM. For fusion index,15 mM/ml D-glucose = 18.15% ± 7.77, 10 mM/ml D-glucose = 20.13% ± 15.18 and 5 mM/ml D-glucose = 21.17% ± 11.22 each vs control DM= 6.979 ± 3.672 showed significance with P value of (0.0001), (< 0.0001) and (< 0.0001) respectively. Further, for calculated myotube area the results were significant only between DM = 5.73% ± 2.04 vs 15 mM/ml D-glucose= 28.03% ± 9.78, (p= 0.0088). Finally, the aspect ratio result confirms significant difference between the control DM= 12.01 ± 7.03 vs each of the treatments respectively; 15 mM/ml D-glucose = 6.57 ± 2.52 (p= 0.0165), 10 mM/ml D-glucose = 6.344 ± 1.03 (p= 0.0138) and 5 mM/ml D-glucose = 4.70 ± 1.16 (P= 0.0008). Overall the fluorescence immunohistochemistry imaging showed normal myotubes formation with aligned nuclei in culture treated with controls (illustrate in figure 11; image A, B &C), while in D-glucose treated myotubes exhibited a significant myotubes morphological abnormalities with centrally clustering nuclei indicated by the red arrows in Figure 11; image D, E & F.

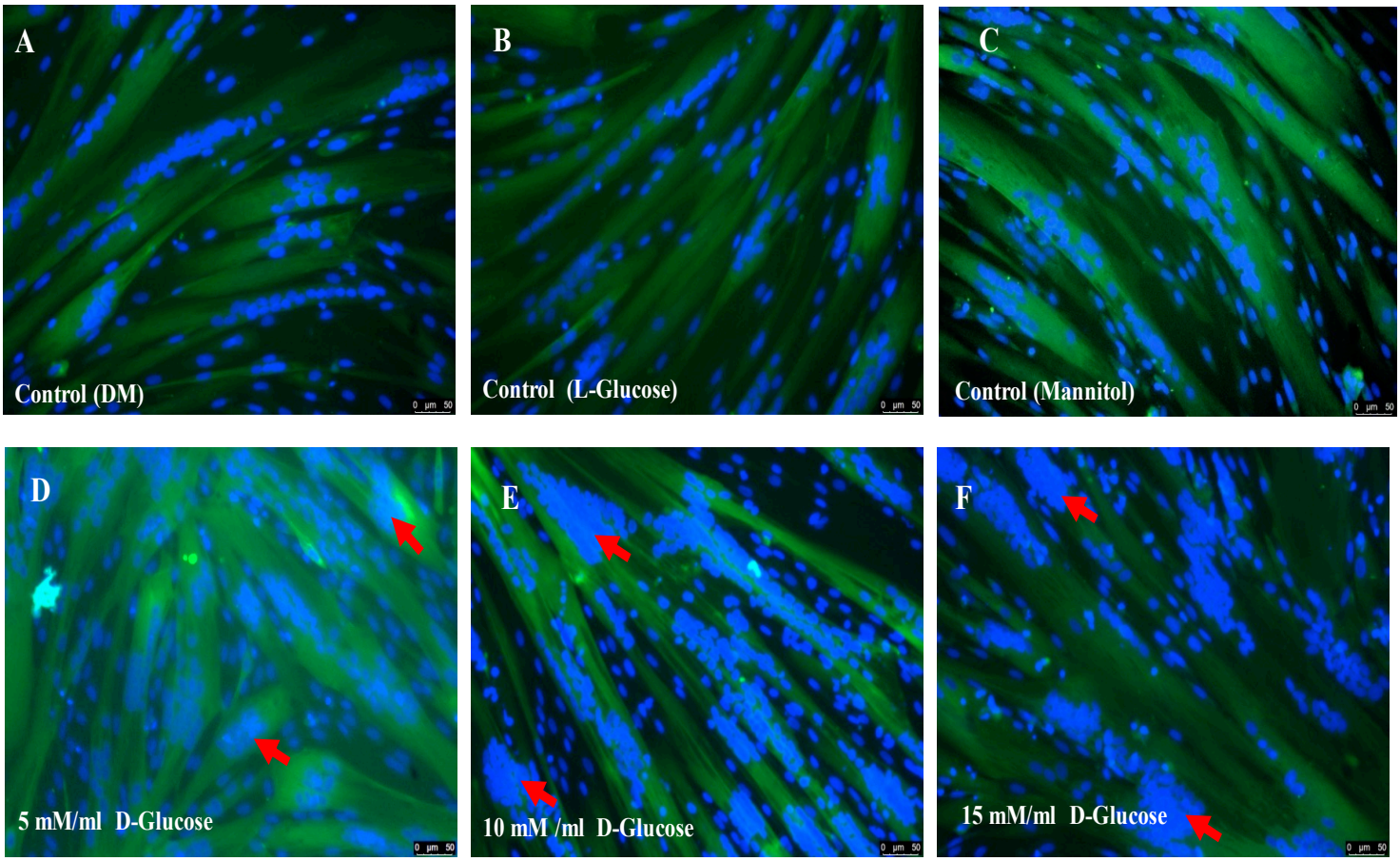

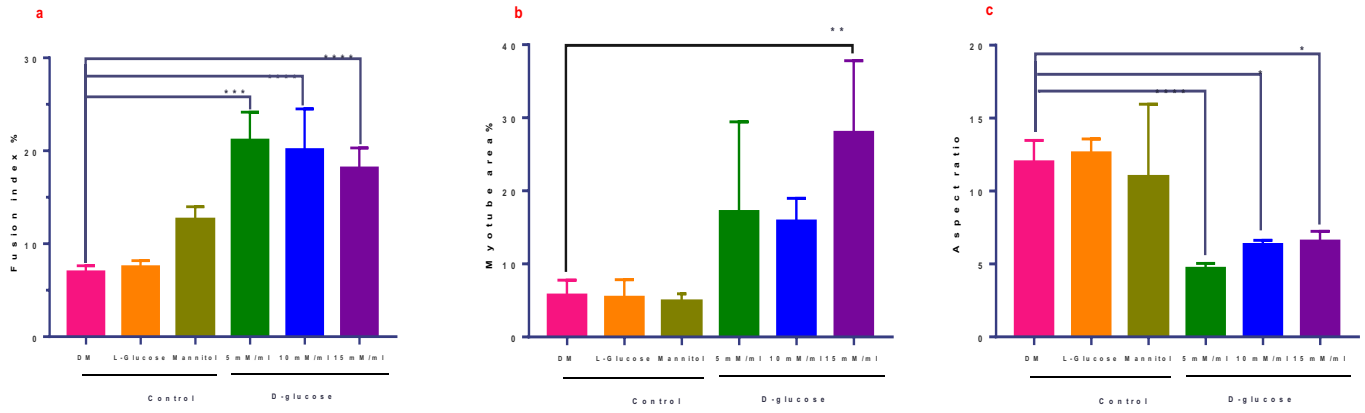

Figure 11: Differentiation parameters of C25 SkMC monoculture following glucose treatment at 96 hours. Image A, B and C display representative overlay of SkMC monoculture showing morphological differentiation of controls DM,L-Glucose (15 mM/ml) and Mannitol (15 mM/ml) respectively. Image D, E and F display representative overlay of SkMC monoculture showing morphological differentiation following treatment with different concentration of D-glucose (5, 10 and 15 mM/ml). The fluorescence immunohistochemistry imaging showed normal myotubes formation with aligned nuclei in culture treated with controls, while significant myotubes morphological abnormalities with centrally clustering nuclei (red arrow) were observed in D-Glucose treated cells (D, E and F). Differentiation parameters (a) fusion index, (b) myotube area, and (c) aspect ratio were measured using immunofluorescent images generated via nucleus stained with DAPI (blue) and myotubes stained with Alexa Fluor-488-MyHC (green), to quantify any significance differences in the differentiation of treated SkMC at 96 hours . Images were captured at 20x magnification. Data are means ± SD of 4 independent experiments.

3.2 Monoculture treatment with AGEs:

3.2.1 SkMC Monoculture differentiation parameters:

Differentiation parameters like fusion index, myotube area, and aspect ratio were measured using immunofluorescent images generated via DAPI nuclear counterstain and MyHC, to quantify any significance differences in the differentiation of treated SkMC at 96 hours with different concentration of AGEs (50µg/ml -200µg/ml) and controls DM/BSA (150µg/ml).The first set of analyses investigated fusion index between DM and different concentrations of AGEs, a significant difference (P = 0.0006) was observed between DM= 6.97% ± 3.67 vs 100 µg/ml = 19.69% ± 10.93, Interestingly, DM vs 150µg/ml =16.33±9.77 and 200µg/ml= 20.8 ± 19.11 there were also significant with (P = 0.0110) and (0.0001) respectively. Nevertheless, there was no significant differences between DM vs 50µg/ml. The aspect ratio analysis results confirmed significant difference between the control DM= 14.59 ± 8.39 vs each of the treatments respectively; 200 µg/ml = 8.84 ± 4.56 (p= 0.0017), 150 µg/ml = 7.77 ± 4.44 (p= <0.0001) and 100 µg/ml = 9.58 ± 7.45 (p= 0.0126). Additionally, no significant difference was observed in DM vs 50µg/ml. On the contrary, calculated myotube area analysis did not show any significant differences between DM and all of AGE treatments. Overall The fluorescence immunohistochemistry imaging showed normal myotubes formation with aligned nuclei in control cultures (illustrate in figure 12; image A & B), while significant myotubes morphological abnormalities with centrally clustering nuclei were observed in AGEs treated cells indicated by the red arrows in Figure 12; image C, D, E & F.

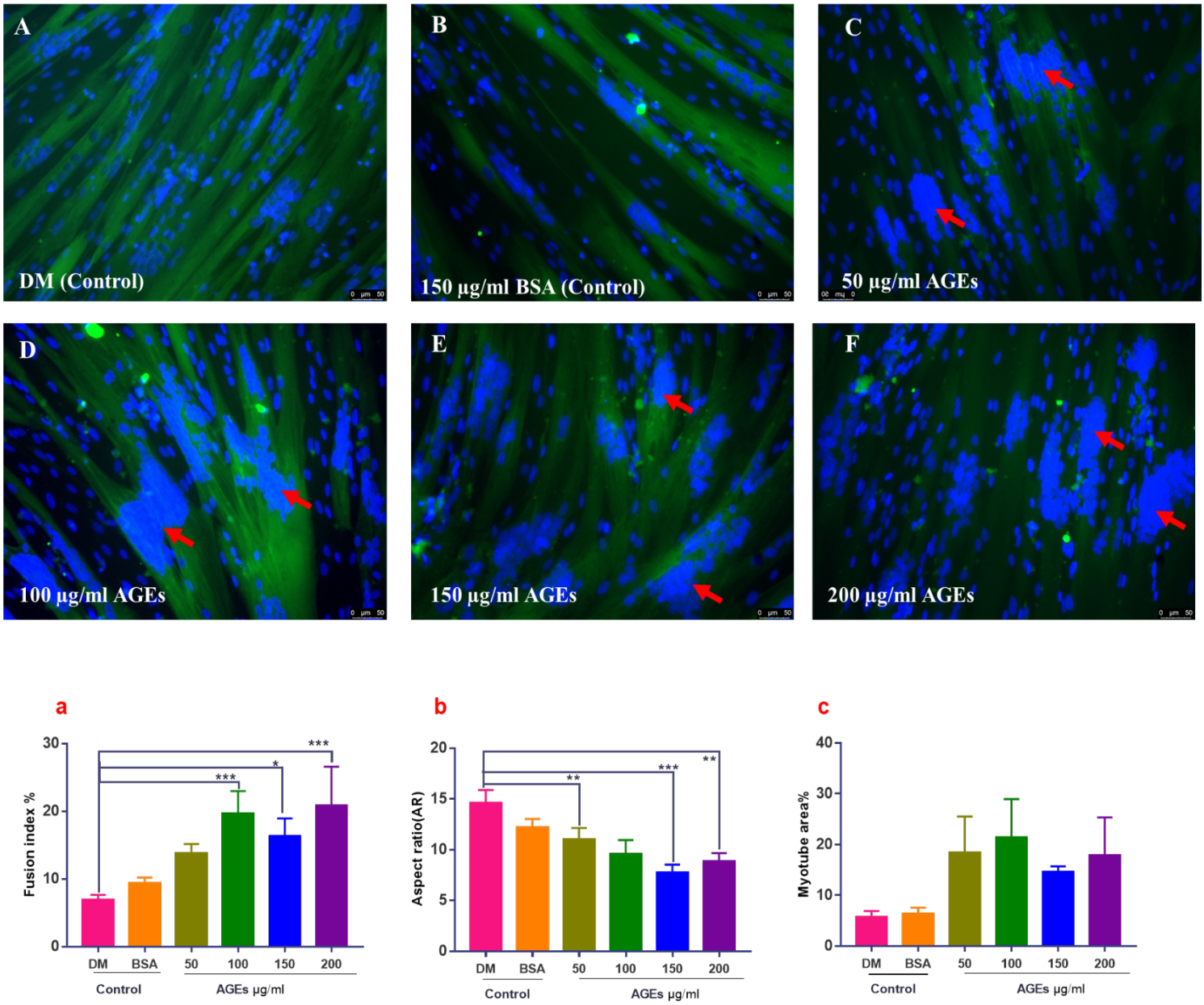

Figure 12: Differentiation parameters of C25 SkMC monoculture following AGEs treatment at 96 hours. .

Image C, D, E and F display representative overlay of SkMC monoculture showing morphological differentiation following treatment with different concentration of AGEs (50, 100, 150 and 200µg/ml) respectively. The fluorescence immunohistochemistry imaging showed normal myotubes formation with aligned nuclei in control cultures, while significant myotubes morphological abnormalities with centrally clustering nuclei (red arrow) were observed in AGEs treated cells (C, D, E and F). Image (A) and (B) display overlay of SkMC monoculture showing morphological differentiation of controls DM and BSA (150µg/ml) respectively. Differentiation parameters (a) fusion index, (b) myotube area, and (c) aspect ratio were measured using immunofluorescent images generated via nucleus stained with DAPI (blue) and myotubes stained with Alexa Fluor-488-MyHC (green), to quantify any significance differences in the differentiation of treated SkMC at 96 hours. Images were captured at 20x magnification. Data are means ± SD of 4 independent experiments.

3.2.2 Mitochondrial Oxygen consumption rate analysis

From the consequent bioenergetics profiles, detailed information can be obtained on the individual elements of the respiratory chain. Ultimately, six mitochondrial function parameters were calculated from the bioenergetics profile (illustrated in Figure 13; image A, B, C, E & F). After OCR measurement, data was automatically displayed by Seahorse XF Mito Stress test report generator.

Estimation of mitochondrial respiration by quantifying OCR of SkMC in monoculture at 96 hours of differentiation treated with different concentrations of AGEs (50-200 µg/ml) or DM/BSA (150 µg/ml) as controls. The baseline OCR of SkMC between the control DM= 36.33 ± 1.37 and AGEs treated cells did not show any significant difference ($P = 0.333$). Further, the calculated Non-mitochondrial respiration showed higher oxygen consumption for cells treated with 150 µg/ml AGEs, however none of these treatments were significant enough ($P \geq 0.3788$) when compared with control DM= 55 ± 4. Although, the OCR results at Basal respiration for cells treated with 150 µg/ml and 200 µg/ml AGEs showed deviation from the mean control value there was no significance difference obtained in of any AGEs treatment. Similarly, the analysis did not confirm any significant differences for Maximal respiration calculated OCR values between the control and all AGEs treated cells. Spare respiratory capacity also showed no significant changes between the control and AGEs treated cells; 50 µg/ml, 150 µg/ml. Furthermore, negative SRC values obtained for 100 µg/ml, 200 µg/ml were excluded from calculation for the purpose of data integrity. Even though, ATP production showed higher variation in OCR between the control and treatment groups, there was no significant difference detected ($P \geq 0.3094$). Interestingly the most remarkable correlation was observed in Proton leak OCR values, showing significance difference for 150 µg/ml AGEs treated cells= 38 ± 4 ($P= 0.0179$) compared with control DM=23 ± 2.

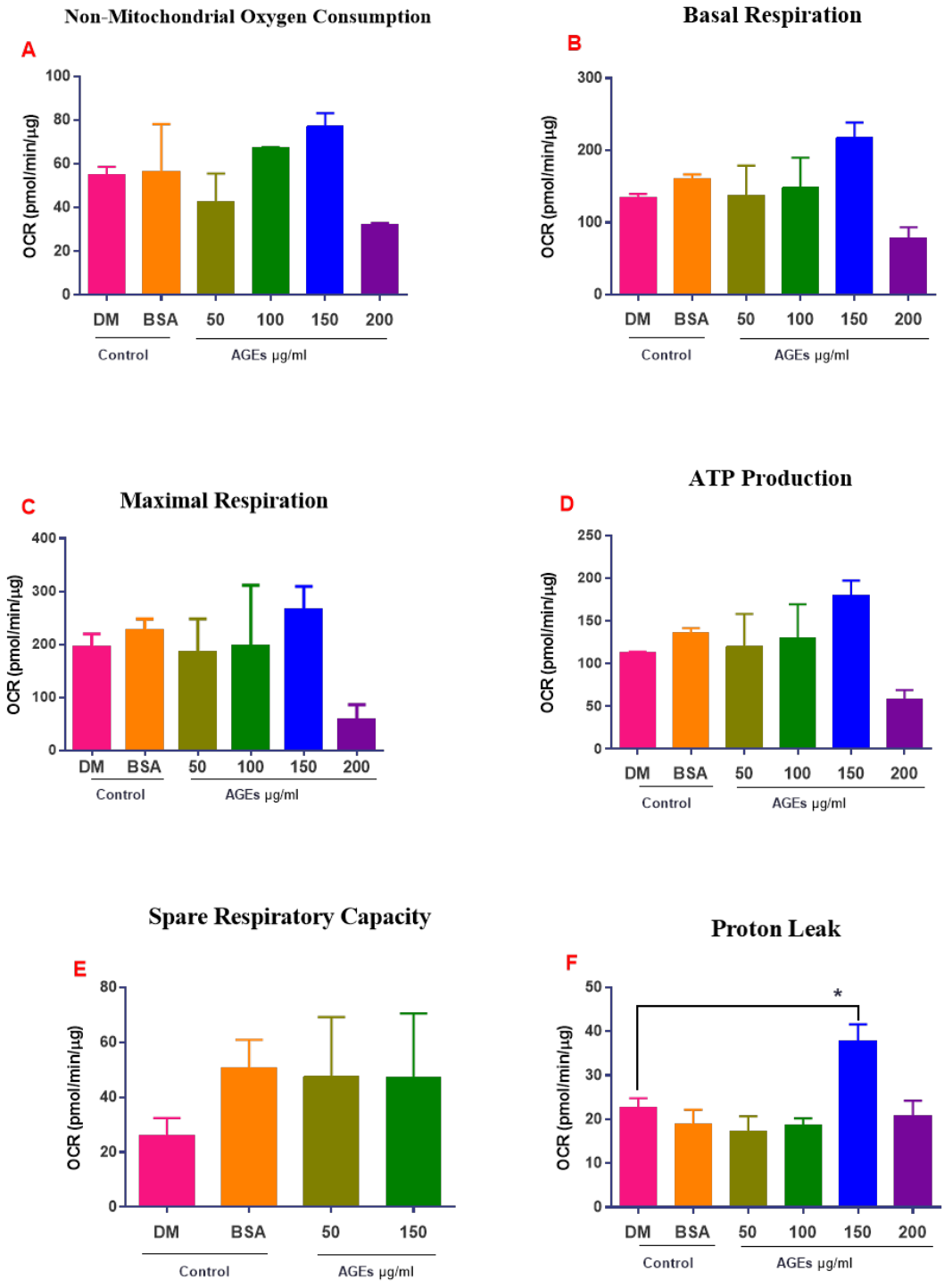

Figure 13: Estimation of mitochondrial respiration parameters of SkMC in monoculture following AGEs treatment at 96 hours. Mitochondrial function parameters that were calculated from the bioenergetics profile: (A) Non-mitochondrial respiration, (B) basal respiration, (C) maximal respiration, (D) ATP production, (E) spare respiration capacity, and (F) proton leak. Estimation of mitochondrial respiration by quantifying OCR of SkMC in monoculture differentiation following treatment with different concentrations of AGEs (50-200 µg/ml) or DM/BSA (150 µg/ml) as controls. Among all these measurements only proton leak OCR values, showed significance difference for 150 µg/ml AGEs treated SkMC (P= 0.0179) compared with control DM. Data are means ± SD of 3 independent experiment.

Ultimately, although AGEs treated SkMC does show a small variation in OCR across measured parameters (Figure 14), the statistical analysis fail to establish a significant difference in most of OCR measurements compared to the control. Overall, Cells that were treated with 150 µg/ml AGEs showed visible changes in OCR in contrast to the lesser concentration of AGEs treatments when compared to the control.

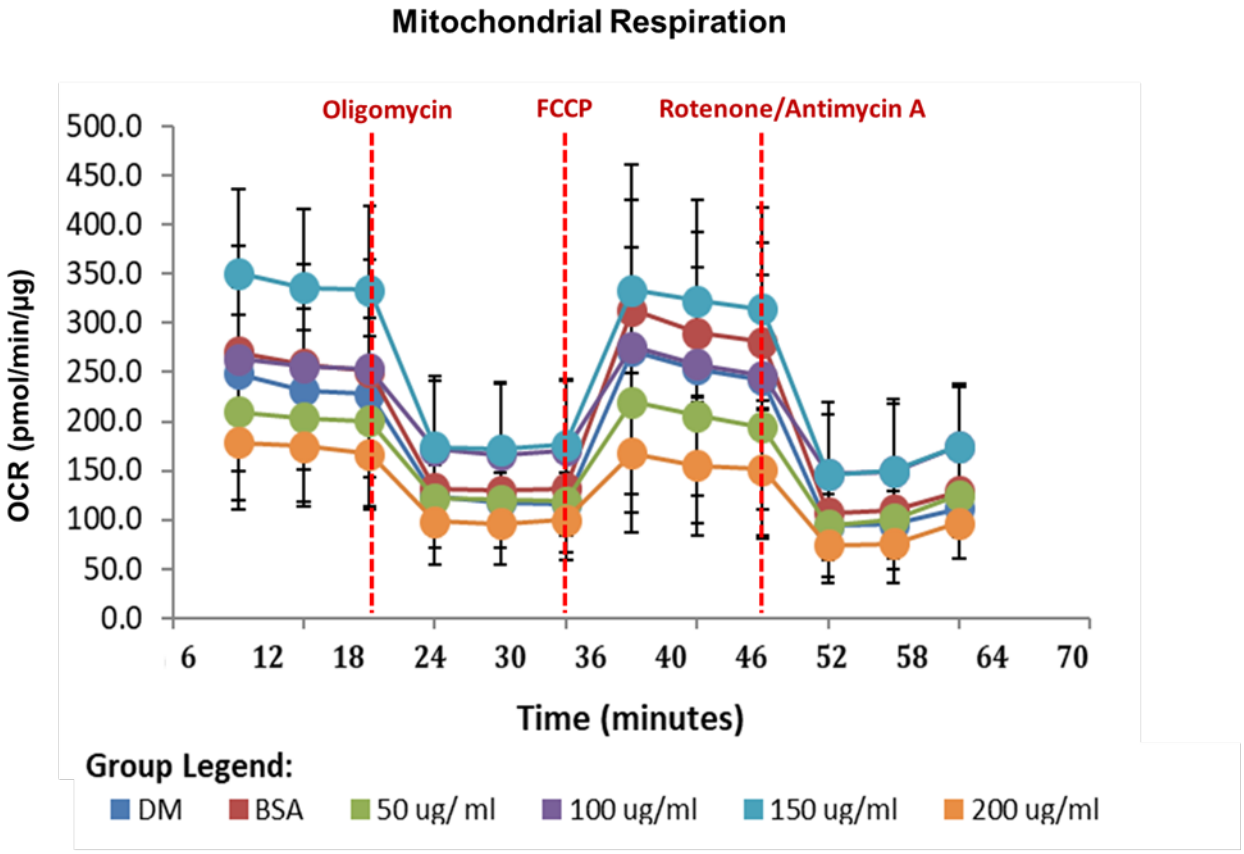

Figure 14: Oxygen consumption rate in SkMc following AGEs treatments with different AGEs concentrations (50, 100,150 and 200 µg/ml) and a control groups (DM and BSA 150 µg/ml).
Twelve OCR measurements were taken in total after sequential compound injections; 3 Basal respiration, 3 oligomycin sensitive respiration (ATP production, 3 maximal respiratory capacity and 3 non-mitochondrial respiration). Over all OCR values decreased with increased AGEs concentration. Data are means ± SD of 3 independent experiment.

3.3 Coculture results:

3.3.1 Coculture morphological phenotypic characterisation

NMJs coculture model was treated with 50-200ug/ml of AGEs and the control BSA over 7 days of differentiation. This was then followed by a staining of the myotubes using Texas Red-X Phalloidin and DAPI. In order to monitor NPCs differentiation into motor neurons GFP-reporter lentivirus system were used. Using the Leica DMI6000 B inverted microscope the stained cells were assessed at 20X magnification consisting of at least five random fields of view selected.

Detrimental effects were observed on myotubes formation and on motor neurons differentiation on cells treated with AGEs. The fluorescence immunohistochemistry imaging showed normal myotubes formation with aligned nuclei in coculture treated with the control BSA, while significant myotubes morphological abnormalities with distinct increase in myotube area and centrally clustering nuclei was observed in all treated myotubes (50-200 ug/ml) indicated by the white arrows in Figure 15; image A1, B1, C1 & E1. Furthermore, in treated NMJs system, less differentiation of motor neurons with shorter axonal formation were observed cells indicated by the red arrows in Figure 15; image A2, B2, C2 & E2. Overall, these images depicted remarkable muscle morphological abnormalities, centrally clustering nuclei, less motor neurons differentiation and shorter axonal formation was observed compared with controls.

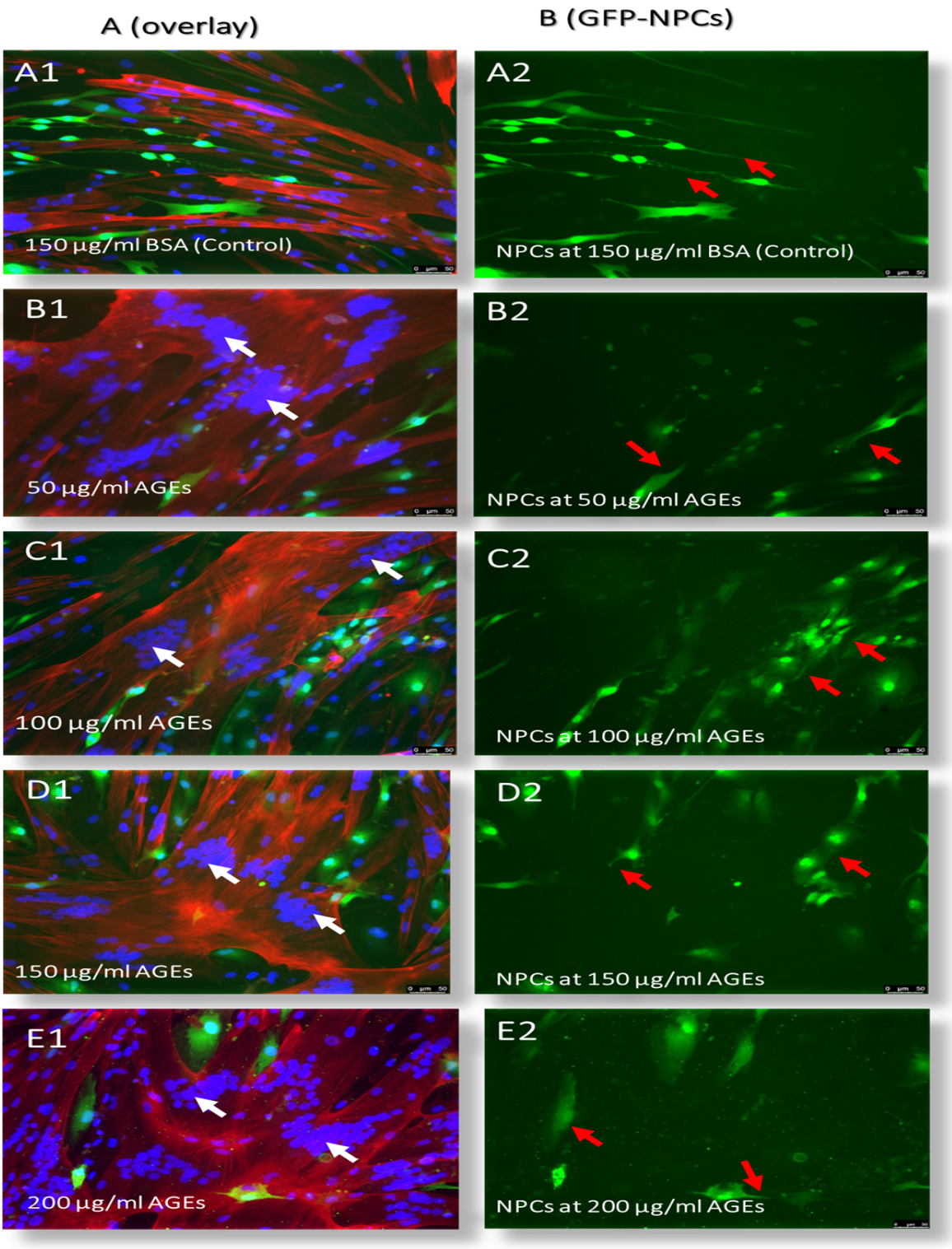

Figure 15 : SkMC coculture morphological characterisation at day 7 of differentiation following AGEs treatments with different AGEs concentrations and a control group.

Image A1, B1, C1, D1 and E1 of panel (A) display representative overlay of coculture showing morphological differentiation treated with the control BSA (150 µg/ml), AGEs 50, 100, 150 and 200 µg/ml respectively. Myotubes stained with Texas Red-X Phalloidin(red) and nucleus stained with DAPI (blue). Image A2, B2, C2, D2, and E2 of panel (B) show GFP-NPCs (green) from the overlaid images of panel (A). The fluorescence immunohistochemistry imaging showed normal myotubes formation with aligned nuclei in co-culture treated with BSA (A1), while significant myotubes morphological abnormalities with distinct increase in myotube area and centrally clustering nuclei (white arrow) was observed in AGEs treated myotubes (B1,C1,D1 &E1). Less differentiation of motoneurons with shorter axonal formation (red arrow) were observed (B2, C2, D2 & E2) compared to control(A2). Images were captured at 20x magnification consisting of at least five random fields of view selected.

3.2.2 *Measurement of axon growth in coculture(nerve-muscle)*

The axonal length of differentiated motor neurons *in vitro* nerve-muscle coculture treated with AGEs were measured over 7 DIV using Image J. The degree of differentiation of motor neurons with regards to AGEs (50-200 µg/ml) treatments or BSA (150 µg/ml) and DM as controls were stipulated using the measured axonal length(µm) in every 24hrs interval. Due to insufficient data, 200 µg/ml AGEs treatment data was not included for day1 to day 6.

In the first set of analysis the axonal length calculated on day-1 showed slight variance with decreased axonal length (indicated by the red arrows in panel (B) Figure 17) yet no statistical significance overall was obtained within 24hrs of differentiation (Figure 16).

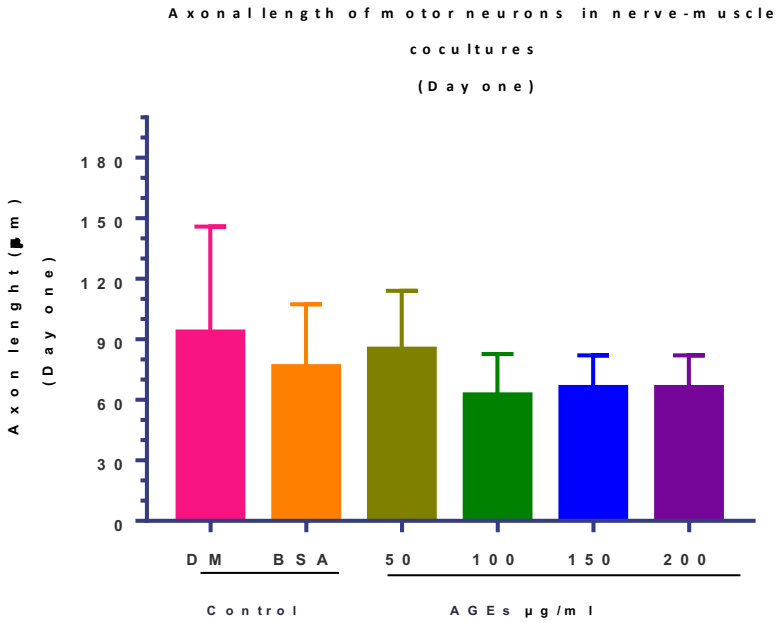

Figure 16 : Quantitative analysis of axonal length in SkMC coculture at 24 hours of differentiation. Four images taken from a representative co-culture were analysed for axonal length at each treatment. No statistical significance in the calculated axonal length (µm) at 24hrs of differentiation following AGE treatments compared to the control groups. Data are means ± SD.

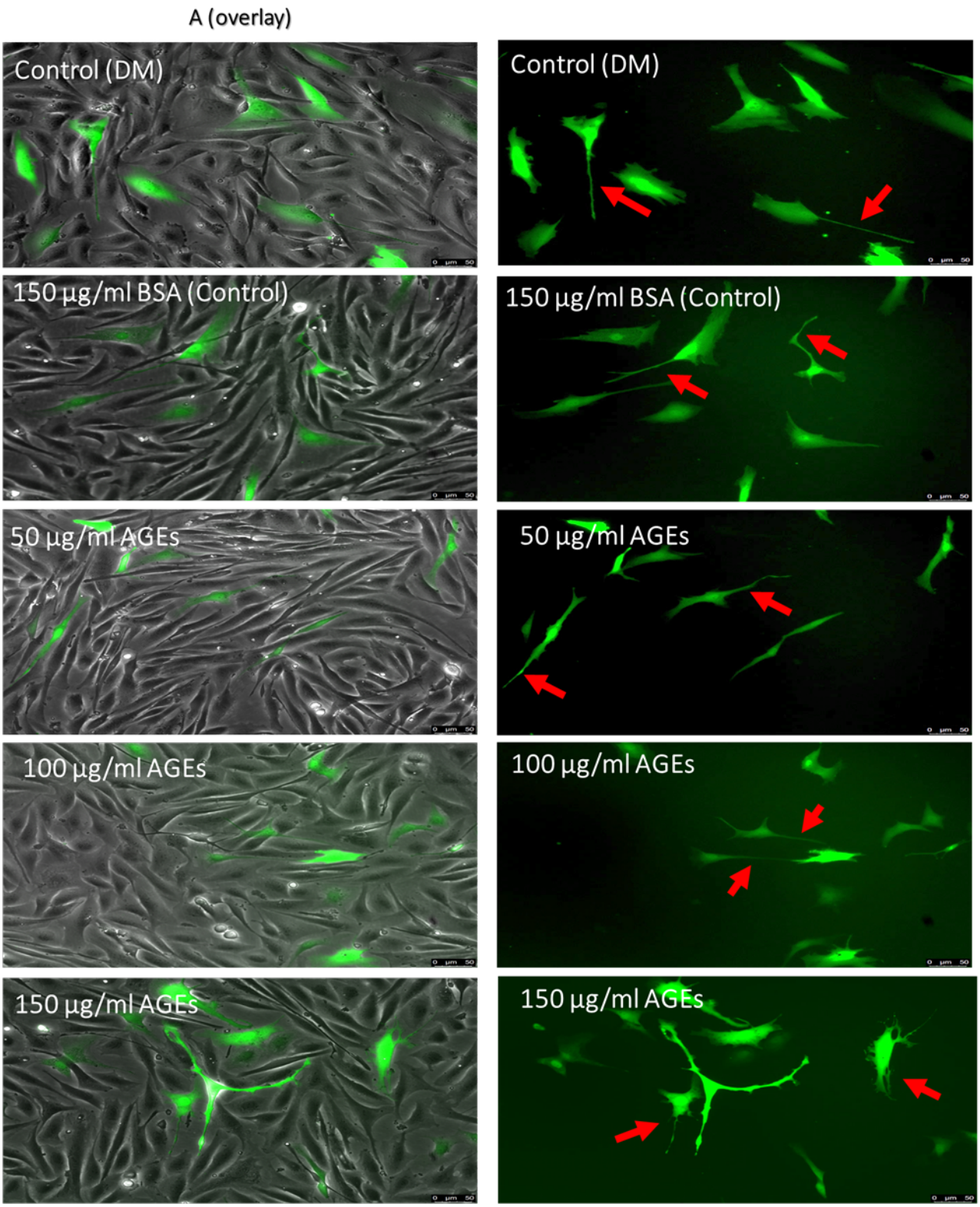

Figure 17: Axonal growth and innervation of differentiated myotubes in AGE treated coculture at 24 hours of differentiation. Image Panel (A) display the overlay pf representative morphology of SkMC myotube (grey) and GFP-motor neurons (green) in coculture for DM and BSA 150µg/ml controls, AGE treatments (50, 100 & 150 µg/ml) at day one of culture. Additionally, image panel (B) show morphology of GFP-NPCs (green) for the same concentrations from the overlaid images of panel (A). No Significant decrease in axonal length (red arrow) was observed on day one of culture in AGE treated cells compered to control groups. Images were captured at 20x magnification.

On the contrary the axonal length calculated on day-7 showed high variance with remarkable decrease of axonal length indicated by the red arrows in panel (B) Figure 19. All concentrations of AGE treatments showed significant difference with P value <0.0001, 50 µg/ml= 125 ± 48.1, 100 µg/ml= 52.59 ± 11.29, 150 µg/ml= 35.28 ± 8.177, 200 µg/ml= 36.45 ± 11.68 compared to control DM = 183.2 ± 81.8 and BSA= 157.7 ± 50.2 (Figure 18).

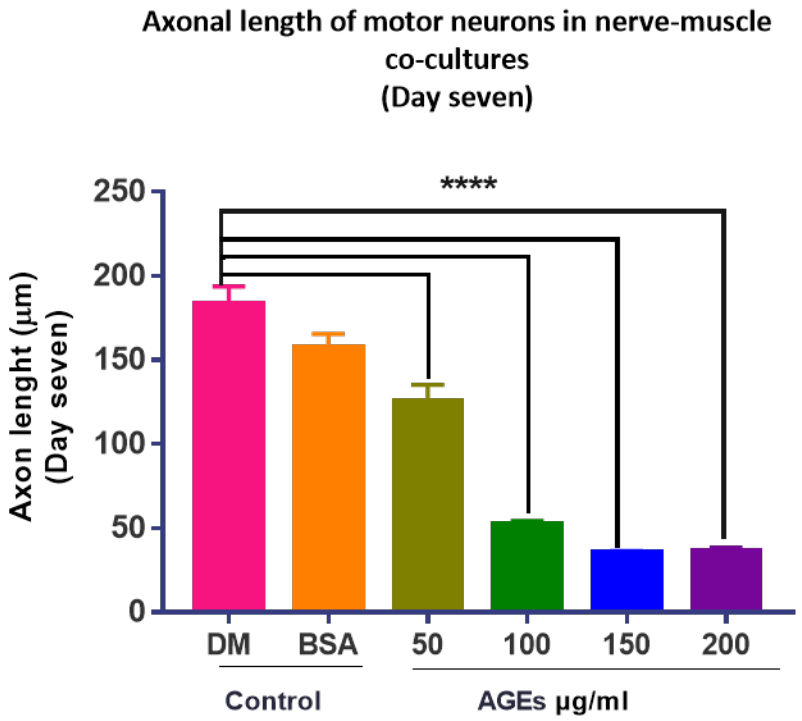

Figure 18: Quantitative analysis of axonal length in SkMC coculture at day 7 of differentiation. Four images taken from a representative co-culture were analysed for axonal length (µm) at each treatment. At day 7 of culture all concentrations of AGE treatments showed Significant decrease in axonal length with P value <0.0001. Data are means ± SD.

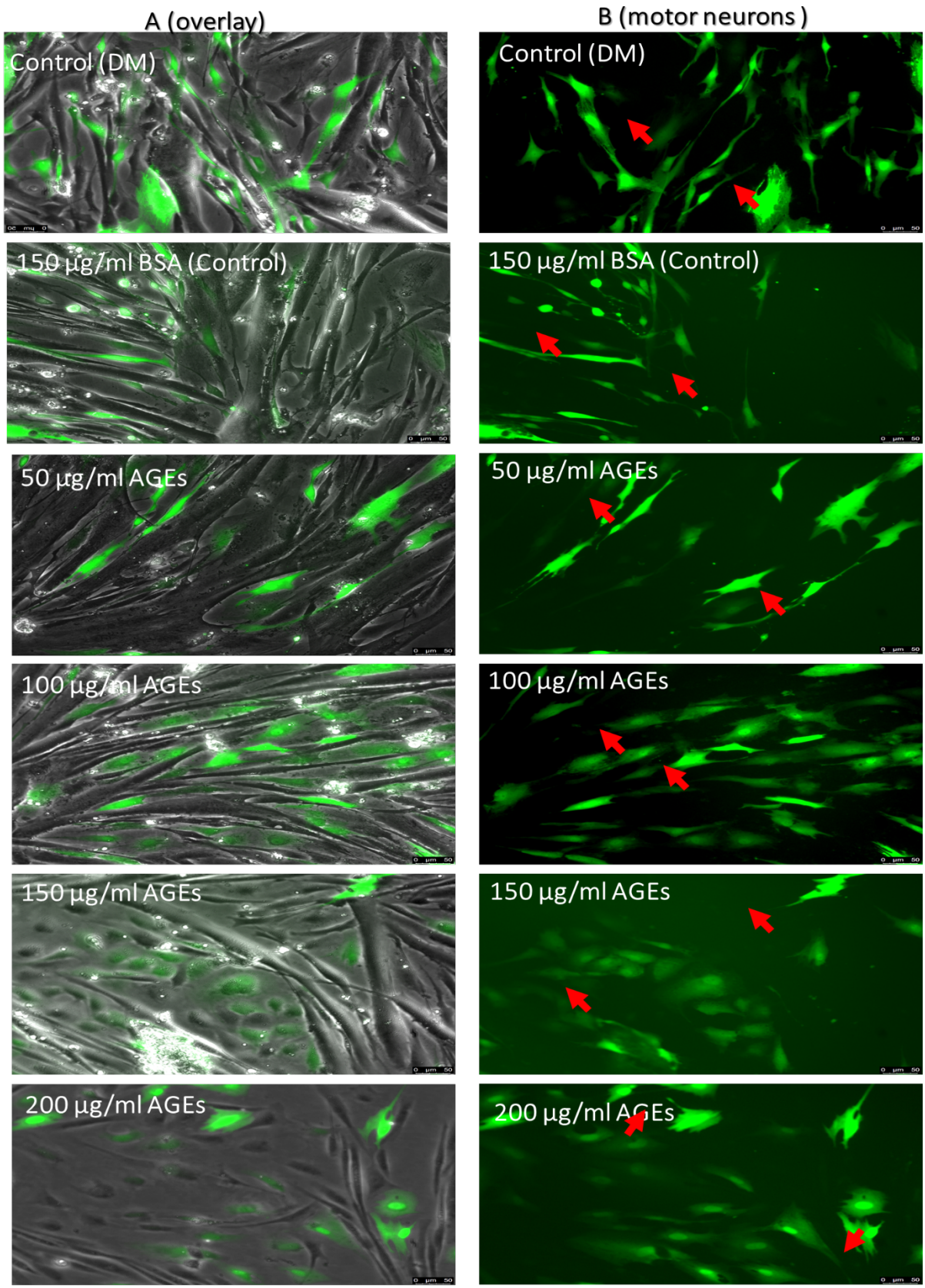

Figure 19 : Axonal growth and innervation of differentiated myotubes in AGE treated coculture at day 7 of differentiation. Image Panel (A) display the overlay of representative morphology of SkMC myotube (grey) and GFP- motor neurons (green) in coculture for DM and BSA 150µg/ml controls, AGE treatments (50,100 & 150 µg/ml) at day 7 of culture. Additionally, image panel (B) show morphology of GFP- motor neurons (green) for the same concentrations from the overlaid images of panel (A). Significant decrease in axonal length (red arrow) was observed on day 7 of culture in AGE treated cells compered to control groups. Images were captured at 20x magnification.

Lastly the axonal length of differentiated motor neurons was measured at each time point over the 7 days of culture for all treatments (Figure 20). Moreover, AGE treated cells showed significance difference in axonal length compared to controls DM and BSA. The axonal length decreased with increased concentration of AGEs treatment over the 7 DIV culture period. The obtained P value for 50, 100, 150 µg/ml was ≤ 0.013.

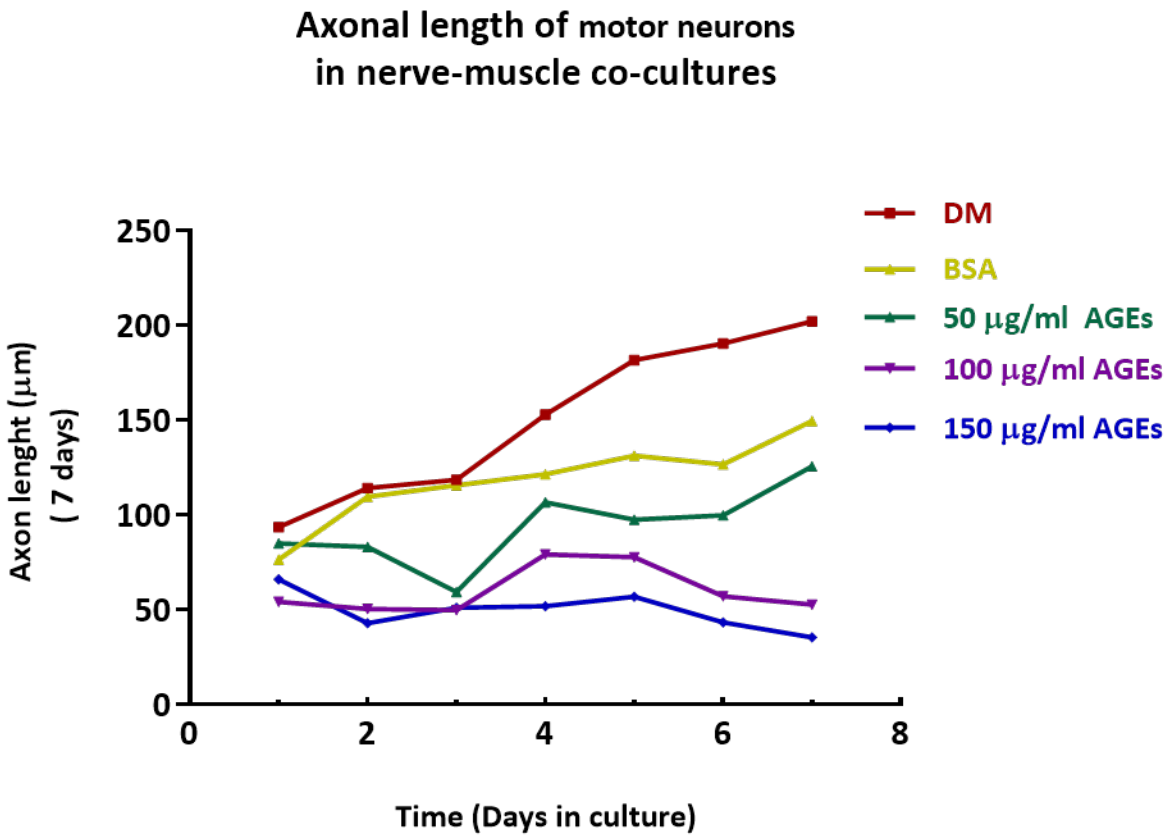

Figure 20: Quantitative analysis of axonal length in SkMC coculture over 7 days of differentiation. Four images taken from a representative coculture and were analysed for axonal length (µm) at each time point over the 7 days of culture for all treatments. The line graph illustrates the calculated axonal length(µm) on Y-axis vs the differentiation time (in days) on X-axis with respect to different concentrations of AGEs treatments in coculture. The axonal length decreased with increased concentration of AGEs treatment compared to the controls DM and BSA over the 7 days in vitro culture (P ≤0.013).

3.3.3 Mitochondrial Oxygen consumption rate analysis

Estimation of mitochondrial respiration of nerve-muscle cocultures cells by quantifying the oxygen consumption rate (OCR) at day 7 of differentiation, treated with different concentrations of AGEs (50-200 µg/ml) or BSA (150 µg/ml) and DM as a control (illustrated in Figure 21; image A, B, C, E & F). The baseline OCR, Non-mitochondrial respiration, Proton leak OCR value of nerve-muscle coculture treated with AGEs did not showed any significance when compared to control DM.

On the contrary Maximal respiration calculated OCR values confirmed significant difference between the control DM= 324 ± 36.5 vs each of the treatments respectively; 200 µg/ml = 205 ± 41.88 (p= 0.0097) and 150 µg/ml = 225.7 ± 24.34 (p= 0.0283). whereas there was no significant difference between DM and other AGE treatments ;100 µg/ml and 50 µg/ml. Similarly, Spare respiratory capacity also showed significant changes only between the control DM = 330.4 ± 28.8 and AGEs treated cells; 150 µg/ml= 121.7 ± 13.98 with P value of (0.0040) and 200 µg/ml= 131 ± 29.58 (p= 0.0082).

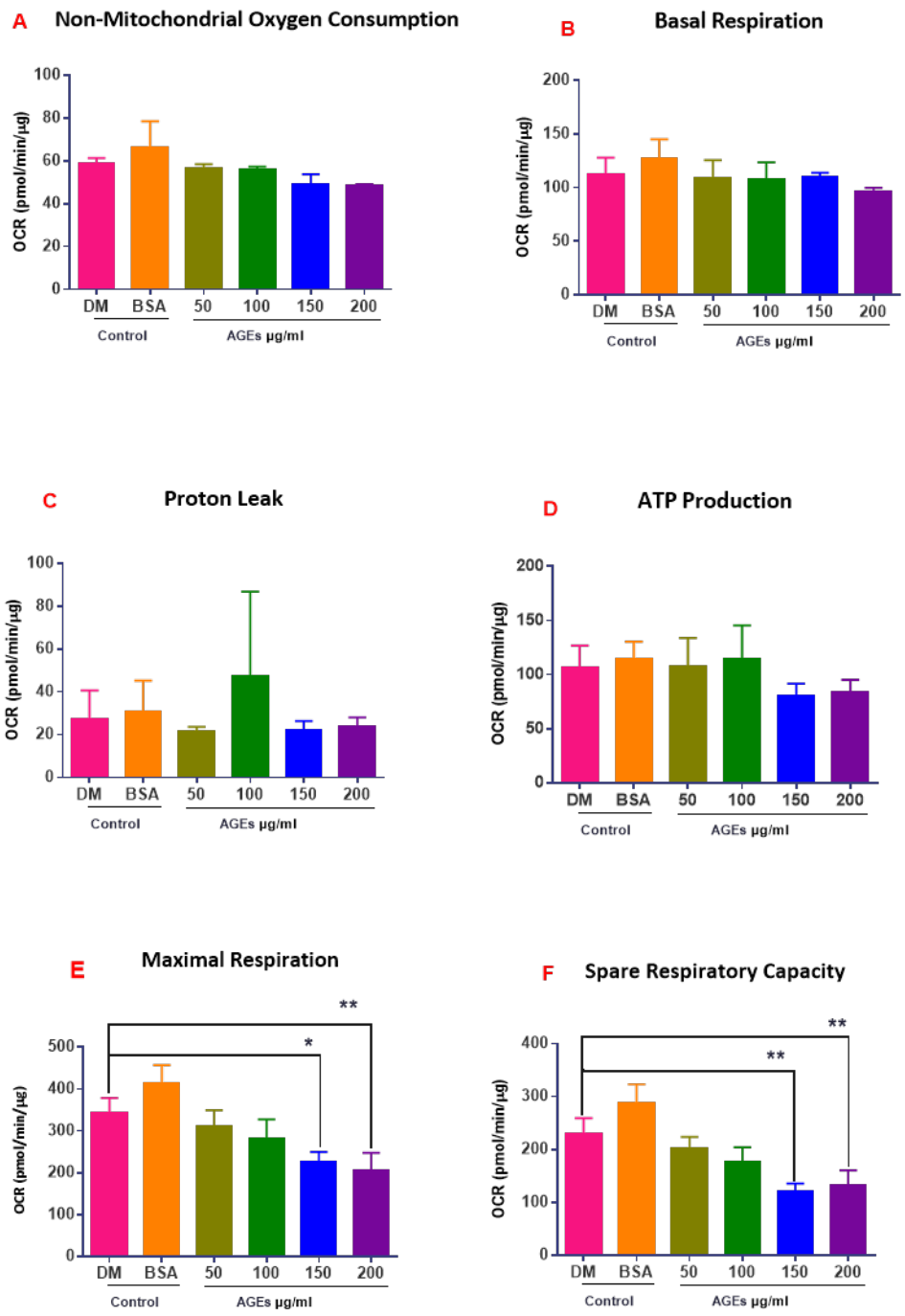

Figure 21: Estimation of mitochondrial respiration parameters of nerve-muscle cocultures cells at day 7 of differentiation. Mitochondrial function parameters were calculated following coculture treatment with different concentrations of AGEs (50-200 µg/ml) or DM/BSA (150 µg/ml) as controls from the bioenergetics profile: (A)Non-mitochondrial respiration, (B) basal respiration, (C) proton leak, (D) ATP production, (E) maximal respiration and (F) spare respiration capacity. Calculated OCR values for (E) Maximal respiration confirmed significant difference between the control DM= 324 ± 36.5 vs each of the treatments respectively; 200 µg/ml = 205 ± 41.88 (p= 0.0097) and 150 µg/ml = 225.7 ± 24.34 (p= 0.0283).(F) Similarly, Spare respiratory capacity also showed significant changes only between the control DM = 330.4 ± 28.8 and AGEs treated cells; 150 µg/ml= 121.7 ± 13.98 with P value of (0.0040) and 200 µg/ml= 131 ± 29.58 (p= 0.0082). Data are means ± SD of 3 independent experiment.

Altogether, SkMC and motor neurons coculture cells showed significant difference in OCR for parameters like Maximal respiration and Spare capacity for 150 µg/ml and 200 µg/ml of AGEs treated cells compared to the control (Figure 22). This obtained significant differences can be extrapolated and studied for further impact of AGEs on mitochondrial respiration of coculture model.

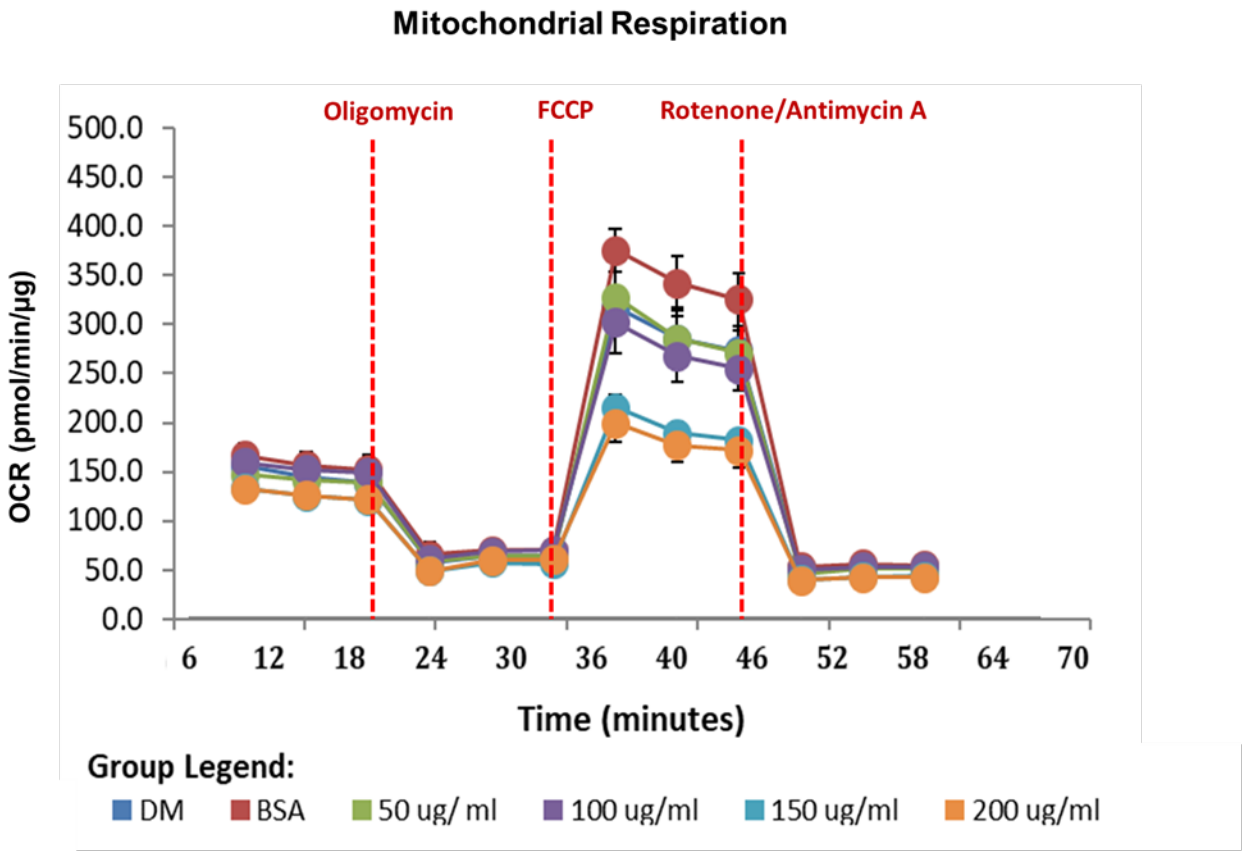

Figure 22: Oxygen consumption rate of nerve-muscle cocultures following AGEs treatments with different AGEs concentrations (50, 100,150 and 200 µg/ml) and a control groups (DM and BSA 150 µg/ml). Twelve OCR measurements were taken in total after Sequential compound injections; 3 Basal respiration, 3 oligomycin sensitive respiration (ATP production, 3 maximal respiratory capacity and 3 non-mitochondrial respiration). Over all OCR values decreased with increased AGEs concentration. Data are means ± SD of 3 independent experiment.

4. Discussion

A number of studies have demonstrated evidence of high levels of glucose and AGEs in diabetes, which interfere with the growth and maintenance of human skeletal muscles (Sango et al., 2017; Hunt et al., 2015; Chiu et al., 2015; Nedachi et al., 2008). However, little is known about the mechanisms controlling muscle cell growth under high glucose and AGEs treatment. Therefore, this study aimed to investigate the adverse impact of high glucose on SkMC and AGEs on skeletal muscle differentiation and NMJ functioning in serum free DM, as serum might contain numerous unknown biological factors which may affect assay reproducibility.

The first set of data illustrated SkMC monoculture treated with different glucose levels, and the subsequent effects on differentiation of muscle cells which were demonstrated by differentiation parameters obtained after immunohistochemistry analysis. Noticeable changes in morphology and calculated differentiation parameters in treated culture compared to the control group were observed. The second set of data illustrated SkMC monoculture treated with different AGEs levels, similar effects were observed in treated culture compared to control groups. Additionally, mitochondrial oxygen consumption rate was measured for AGEs treated SkMC monoculture and the primary impact was seen in OCR values for proton leak which indicates impaired mitochondrial membrane potential.

The final set of analysis were carried on the novel nerve-muscle coculture model with serum and neural growth factors free media. Moreover, the absence of neural growth factors from the coculture model suggests that nerve and muscle cells release all the required factors needed to stimulate nerve axonal developing and formation of NMJs with myotubes. Overall the simplicity of this novel model makes it ideal for high-throughput researches that may affect NMJ formation and myotube differentiation. The data for this model demonstrated similar effects in morphology as observed in SkMC monoculture cells and decreased axonal length of cultured motor neurons following treatment with AGEs. Next the impact of AGEs on mitochondrial oxygen consumption rate was measured by calculating OCR parameters. From the results, it was clear that OCR values for maximum respiration and spare capacity were significant compared to controls in coculture model suggesting potential mitochondrial damage and dysfunction.

Form the first set of analysis it is clear that the presence of high glucose in SKMC monoculture had a remarkable effect on skeletal muscles differentiation, demonstrated by significant difference in fusion index, myotube area and aspect ratio compared to control group (Hunt et al., 2015; Nedachi et al., 2008). This data indicates that these findings could be considered as a toxic effect induced by glucose. In fact, some studies have suggested that the obtained results could resemble *in vivo* mechanism of hyperglycaemia, which ultimately might contribute in insulin resistance (Grabiec et al., 2014; Copeland et al., 2008). These mechanisms eventually cause tissue damage by various metabolic pathways, such as elevated polyol and hexosamine pathways flux, formation of AGEs, stimulation of protein kinase C, and increased production of ROS(Copeland et al., 2008; Howard et al., 2011). Overall, differentiation parameter data and the myotube morphological changes are in accordance with findings reported by (Nedachi et al., 2008; Grabiec et al., 2014; Hunt et al., 2015) as their results stated that when high ambient glucose present extracellularly induces myogenesis in mouse C2C12 myoblast by insulin in low serum media. However, when comparing our results to previous studies (Nedachi et al., 2008; Grabiec et al., 2014; Hunt et al., 2015), point should be considered that in this study, the cells were differentiated in serum free media. Therefore, the effects on differentiation seen in this study were solely from glucose treatment unlike in the above-mentioned studies where the presence of serum can interfere and alter outcomes of the treatment. Moreover, Hunt et al., (2015) stated that increased myoblast fusion is induced by elevated levels of glucose through promoting glucose-responsive transcription factor Max-like protein X activity. From these results it is clear that the high glucose level prompts over-differentiation resulting increased myotubes area and fusion. This implies that the abnormal muscle differentiation is associated with alterations in the expression of muscle genes, which may lead to insulin resistance (Grabiec et al., 2014; Hunt et al., 2015).

It is worth discussing these interesting facts revealed by results of this study that the effect of high glucose prompts over differentiation of myoblast evident by increase in myotubes area and fusion index. In contrast to several studies in the literature (Grzelkowska-Kowalczyk et al., 2012; Grzelkowska-Kowalczyk, 2014) which showed that high glucose treatments had opposing effects that caused decreased myotubes differentiation and fusion. Although reasons for this

discrepancy is not yet clear, it could be due to the use of human cell line in this study whereas animal cell line (C2C12) were used in the mentioned study. Even though, there is still some controversy surrounding the presence of high insulin (10 µg/ml) and glucose (25 mM/l) in DM, it is important to realize that they are essential to stimulate myotube formation and most of the DM glucose is consumed as source of energy for muscle growth and fusion (Nedachi et al., 2008).

For the second set of analysis, following treatment of SKMC monoculture with high AGEs data showed noticeable effect on skeletal muscles differentiation, demonstrated by increase in fusion index and decreased aspect ratio and no effect seen on myotube area compared to control groups. These basic findings are consistent with research showing that AGEs exhibit their effects by binding and activating RAGE (Cassese et al., 2008; Chiu et al., 2015). This initiates cascade of cell signalling pathways like MAPK, cdc42/Rac, ERK1/2, phosphatidylinositol 3-kinase, PKC, the Janus tyrosine kinases (JAKs), and transcription factors, including STAT3, AP1, and NF-κB. These signalling pathways causes the multimolecular complex formation and results in coprecipitation of proteins causing imbalance in the cellular function and regulation (Cassese et al., 2008). Furthermore, other studies have shown that myogenin supress the paired-box 7 (PAX7) transcription by binding to high-mobility group box 1 (HMGB1)– RAGE and PAX7 promoter region. Whereas PAX7 is an important transcription factor that controls myoblast proliferation and differentiation: in excess and prolonged proliferating skeletal muscle cells high levels of PAX7 are present, while in advanced differentiation low levels of PAX7 are expressed. Therefore, increased levels of RAGE downregulate PAX7 signalling pathway causing increased myogenic differentiation (Riuzzi et al., 2012). Thus, in a wider perspective AGEs accumulation and their respective binding domain RAGE has a vital function in inducing pathogenesis of diabetic myopathy and increased generation of ROS, proinflammatory cytokines and adhesion molecules (Chiu et al., 2015).

Overall, to some extend the same effects on differentiation was observed on cultured skeletal muscles following the treatment with high concentrations of glucose (in monoculture) and AGEs (in mono and coculture) compared to the control groups. Myotubes looked deformed with abnormal morphology and random central nuclei clustering, compared to branched and leaner myotubes with aligned nuclei at the periphery in control cultures. Furthermore, many musculoskeletal studies suggested that any alterations in the muscle structure will affect

muscle contraction activity and fibre functionality (Folker and Baylies, 2013; Jungbluth and Gautel, 2014; Tasfaout et al., 2018). During muscle formation the nuclear positioning happens in multiple stages, first myoblast fuse into myotubes and the nucleus move and centralise. Then they spread along the myotube axis and move near to the periphery where they get localised. Moreover, some nuclei gather and cluster (three to eight nuclei) under the NMJ as it is vital for synaptic transmission (Roman and Gomes, 2017). In fact, the myodomains theory have suggested that nucleus positioning within the myotubes are very important as each nuclease have an important role in regulating cellular function of that practical area of the muscle (Folker and Baylies, 2013). However, when the nuclei are centrally clustered, other areas of the muscle will be deprived of the transcriptional and translational end products needed for myofiber sustainability, that could also result in absence of nuclei clustering at the NMJ which is possibly linked to neuromuscular disorders (neuropathy) (Cadot et al., 2015). Normally, myonuclei were located peripherally in a defined manner to maximized distance between each other, while centrally located myonuclei were evident in pathological conditions (Folker and Baylies, 2013). Therefore, account of nuclear mispositioning is a suitable morphological marker and vital during pathological correlation of various muscle disorders (Romero and Bitoun, 2011).

Although, clustering of nuclei in absence of any clear defects can interfere with muscle functioning, the event of nuclear movement and relative gene regulation cannot be accounted as mere reason for neuromuscular diseases. A wider perspective and ample amount of studies are required to understand highly regulated nuclear movements inside myotubes and its essence in appropriate muscle functioning (Folker and Baylies, 2013). Overall these study findings are in accordance with findings reported by the above-mentioned studies which focused on the skeletal muscle morphological variation and their involvement in inducing myopathy and neuropathy which support our hypothesis that high levels of glucose and AGEs have detrimental effects on skeletal muscle myogenic differentiation and nuclear positioning. In fact, this might simulate the development of *in vivo* diabetic complications related to skeletal muscle and NMJ system (Drenth et al., 2016).

For investigating diabetic neuropathy, the coculture model treated with AGEs for 7 DIV showed that healthy motor neurons were affected by AGEs accumulation and this was reflected by decreased motor neurons differentiation, innervation and reduced axonal length compared to control cells. These results tie well with studies that suggest AGEs has neurotoxic effects caused by AGEs/RAGE activity which contribute in elevated free radical's production, oxidative damage and raise mitochondrial permeability eventually leading to apoptosis (Sango et al., 2017; Xing and Zhang, 2013; Zochodne et al., 2008). Furthermore, previous studies propose AGE mainly disrupts neuronal cytoskeleton (King, 2001; Edwards et al., 2008) by protein phosphorylation and increasing the concentration of intracellular phosphorylated messengers (Ahmed, 2005). Where in diabetic patient pentosidine level (biomarker for AGEs) was found increased in myelin and cytoskeletal fractions, this could be an evidence that AGE targets neural cytoskeleton proteins and cause their glycation in neuronal cells of diabetic patients (Öztürk et al., 2006). These modifications of axonal proteins aids in axonal atrophy and degeneration. Thus, glycation of myelin proteins by AGEs expose them to phagocytosis by macrophages and excretion of proteases which may cause nerve demyelination (Trnková et al., 2015). A similar pattern of results was obtained in another study when motor neurones derived from mice subjected to prolonged diabetic condition (Muramatsu et al., 2012; Souayah et al., 2009) showed thinner myelin sheet and decrease in axonal length and reduced motor neuron differentiation leading to abnormalities due to electrophysiological functionality of motor neurons and decrease in conduction velocity (Gonzalez-Freire et al., 2014). However, less morphological changes were observed in animal models with diabetic neuropathy compared to higher neuronal degeneration in human diabetic polyneuropathy (Sango et al., 2017). Moreover, when comparing this present study findings to those of older animal-based studies, it must be pointed out the use of a human based model provides more relevant platform to mimic *in vivo* diabetic conditions in human neuropathy (King, 2001; Höke, 2012; Gonzalez-Freire et al., 2014).

The final analysis of mitochondrial bioenergetics study was performed to investigate the effect of AGEs on the cellular level in both monoculture and coculture models. The analysis of mitochondrial respiration tracks changes in cell bioenergetic parameters by exposing the mitochondria to pathological stress revealing the mitochondrial impairment and functioning

overall. This is achieved by inhibiting oxidative phosphorylation with addition of pharmacological inhibitors (Oligomycin, FCCP, and Antimycin A / Rotenone). Mitochondrial stress assay provided real time mitochondrial function analysis parameters in both monoculture and coculture model showing relative decrease in oxygen consumption parameters stating the impairment in mitochondrial function when treated with AGEs. The OCR value during basal respiration which accounts for the oxygen consumption to replenish cellular ATP requirement under baseline conditions showed no significant changes between the control and treated cells in both models stating the null impact of treatments on cultured cells at this point of experiment. Proton leak OCR values were obtained after treating the cells with ATP synthase inhibitors (oligomycin) which disrupts electrochemical gradient and phosphorylation reactions in mitochondrial membrane. The OCR value for monoculture Proton leak was elevated for cells treated with higher AGEs contractions (150 µg/ml) and showed a significant difference suggesting mitochondrial membrane damage of SkMC cells. On the other hand, nerve-muscle coculture showed high proton leak value for some AGEs treatments there was no significance, yet it might still indicate a membrane damage in nerve and muscle cells. Although the complete mechanism behind the proton leak not clearly understood, positive correlation between proton leak, inner mitochondrial surface area and electron transport chain are established from multiple quantitative studies (Brand and Nicholls, 2011; Sansbury et al., 2011). It has been suggested that this impairment causes leak of H+ into the intracellular matrix or slippage of electron leading to disruption of the proton gradient resulting in higher consumption of oxygen (Sansbury et al., 2011; Porter, 2001; Echtay, 2003). Additionally, the disruption of electron transport chain demonstrated some effect on ATP-linked OCR which could be also linked to proton leak and damaged inner mitochondrial membrane (Sansbury et al., 2011). The addition of uncoupler FCCP cause the cell to undergo respiration at maximum level. This value is noted as maximum rate of respiration. In case of healthy mitochondrial functioning, cell needs to meet higher demand of energy that corresponds to higher OCR for maximum rate of respiration (Dranka et al., 2011). The results for this parameter in SkMC monoculture showed remarkable decrease in 200 µg/ml AGE treated cells compared to the controls, yet it was not significant. However, decrease in maximum capacity for the treated cells (150, 200 µg/m AGE) in the coculture showed significant differences

which may indicate loss of mitochondrial integrity or relative mass. These data imply that AGEs could be associated with mitochondrial dysfunction in muscle and nerves (Hill et al., 2012). The reserve capacity also known as spare respiratory capacity is an important qualitative indicator for accessing the functionality of mitochondria and its status. Various factors that accounts for Spare respiratory capacity value are substrate supply, coupling, ATP demand, mitochondrial mass and its network (Hill et al., 2012). The decreased spare respiratory capacity of the nerve-muscle treated cells compared to control indicates that the mitochondria could not meet the energetic needs of the cocultured cells (Brand and Nicholls, 2011).

On the whole within the motor neurons the axons consist of higher number of mitochondria and are exposed to direct nerve blood supply making them susceptible to hyperglycaemic and AGEs damage (Brownlee, 2001). The damage is initiated within axon as stated by distal-proximal axon length pattern of diabetic neuropathy progression (Leinninger et al., 2006). Superoxide dismutase, catalase and glutathione removes the ROS formed by normal mitochondrial electron transport chain (Edwards et al., 2008). This ability of mitochondria is hindered by excess formation of ROS and reactive nitrogen species due to hyperglycaemia induced cytotoxic effects such as; AGEs production, activation of Poly (ADP-ribose) polymerase pathway (PARP) and protein nitrosylation (Obrosova et al., 2005). This phenomenon effects the functional lipids, proteins and DNA eventually compromising cellular function and integrity (Edwards et al., 2008). Studies have shown that hyperglycaemia induced nerve damage is enhanced by the formation of AGEs and PARP (Ilnytska et al., 2006) where they synergistically increase the cellular oxidative stress, over produce superoxide and inhibits the Glyceraldehyde 3-phosphate dehydrogenase (GAPDH) activity (Vincent and Feldman, 2004). Glycolytic intermediates accumulated due to GAPDH inhibition leads to increased production of the enzyme aldose reductase (AR), Protein kinase C (PKC) and AGEs, eventually causing more cell damage (Wada et al., 2001). Similarly, like neuronal cells, the increased oxidative stress and prolonged low-grade inflammation induced by AGEs in skeletal muscle cells cause the mitochondrial dysfunction (D'Souza et al., 2013). In fact, some studies hypothesised that it all begin with motor unit becoming smaller, followed by decreased nerve innervation which eventually effects the NJM causing atrophy and decrease in muscles fibre number (Gonzalez-Freire et al., 2014; Wilson and

Wright, 2014). All these sequential steps can be linked together with AGEs impact on mitochondria dysfunction which may play major role in inducing diabetic myopathy and neuropathy (Wilson and Wright, 2014).

5. Research limitations

The limitations of the present study include the presence of high glucose levels in the DM which might interfere with glucose treatments. However, it was demonstrated in some studies that elevated glucose levels in DM are essential as source of energy for SkMC cell line growth (Grzelkowska-Kowalczyk, 2014; Nedachi et al., 2008; Grzelkowska-Kowalczyk et al., 2012. In this study differentiation parameters for the myotubes in the coculture were not accessed due to limited availability of unconjugated NPCs, therefore the myotubes were stained using Texas Red-X Phalloidin instead of Fluor-488-MyHC (green) which is essential for studying differentiation parameters. Another limitation in BSA-AGE composition involves the issue of efficient endotoxin removal, although the endotoxins were removed before cell treatment it is controversial that AGEs might still exert endotoxic effects and form lipopolysaccharides by interacting with lipoproteins. Another concern about the findings of oxygen consumption rate in coculture model with two cell types, it is difficult to determine if the results reflect muscle or nerve mitochondrial activity. Nevertheless, many studies had demonstrated that same mechanisms of mitochondrial dysfunction could be involved in both cell types. Lastly, axonal analysis method needs farther standardisation as the use of imageJ software could be subjective.

6. Clinical impacts and future directions

Further study focusing in the biochemical analysis and gene expression/repression mechanism of AGEs/RAGE on skeletal muscle and NMJ functioning can be designed by expanding this novel human platform which will give insight into the *in vivo* mechanism of the impact of AGEs in diabetic conditions and correlation with clinical findings. Not to mention that this model is a functional NMJ platform which could be employed in future to test the effect of hyperglycaemia and AGEs in muscle contraction.

A promising subject of research that has potential to demonstrate the cellular level interaction of Glucose and AGES with Skeletal Muscles and NMJ *in vitro*. The morphological change,

mitochondrial bioenergetics parameters and decreased axonal length support the clinical findings in relation with diabetic myopathy and neuropathy. Discovering the pattern of nuclear movement and its importance during cell proliferation and differentiation can help in clinically corelating the pathophysiological conditions. In depth study of intermediate product of AGES and mode of action of ROS activity in cellular differentiation process and mitochondrial functioning forms the basis for innovative research with human skeletal muscles and neuronal cells, allowing for further knowledge of the mechanism of impact on cell integrity and dysfunction.

7. Conclusions

In conclusion, employment of this novel human-based platform to investigate the potential involvement of glucose and AGEs in the advancement of diabetic myopathy supports the hypothesis of this study, demonstrated by disruption of myotubes morphology and centralised nuclei clumping. Moreover, the results also proved that AGE affected motor neural differentiation and innervation in NMJ model which could play an important role in the development of diabetic neuropathy. Likewise, the mitochondria bioenergetics data can be linked together with AGEs impact on mitochondria dysfunction and their major role in inducing diabetic myopathy and neuropathy. Therefore, the use of NMJ platform in this study contribute in a novel investigation to raise the question where AGEs damage begins? From muscle or nerve. With this in mind further studies needed to answer this question, and this project could be the first step in this path.

8. References

Bentzinger, C., Wang, Y. and Rudnicki, M. (2012) 'Building Muscle: Molecular Regulation of Myogenesis'. Cold Spring Harbor Perspectives in Biology, 4(2) pp.a008342-a008342.

Shadrach, J. and Wagers, A. (2011) 'Stem cells for skeletal muscle repair'. Philosophical Transactions of the Royal Society B: Biological Sciences, 366(1575) pp.2297-2306.

Le Grand, F. and Rudnicki, M. (2007) 'Skeletal muscle satellite cells and adult myogenesis'. Current Opinion in Cell Biology, 19(6) pp.628-633.

Zammit, P., Golding, J., Nagata, Y., Hudon, V., Partridge, T. and Beauchamp, J. (2004) 'Muscle satellite cells adopt divergent fates'. The Journal of Cell Biology, 166(3) pp.347-357.

Chal, J. and Pourquié, O. (2017) 'Making muscle: skeletal myogenesis in vivo and in vitro'. Development, 144(12) pp.2104-2122.

Grounds, M. (1998) 'Age-associated Changes in the Response of Skeletal Muscle Cells to Exercise and Regenerationa'. Annals of the New York Academy of Sciences, 854(1 TOWARDS PROLO) pp.78-91.

Abdul-Ghani, M. and DeFronzo, R. (2010) 'Pathogenesis of Insulin Resistance in Skeletal Muscle'. Journal of Biomedicine and Biotechnology, 2010 pp.1-19.

Kelley, D. and Mandarino, L. (2000) 'Fuel selection in human skeletal muscle in insulin resistance: a reexamination'. Diabetes, 49(5) pp.677-683.

Ahmed, N. (2011) Clinical biochemistry. Oxford;New York;: Oxford University Press.

D'Souza, D., Al-Sajee, D. and Hawke, T. (2013) 'Diabetic myopathy: impact of diabetes mellitus on skeletal muscle progenitor cells'. Frontiers in Physiology, 4.

Mamchaoui, K., Trollet, C., Bigot, A., Negroni, E., Chaouch, S., Wolff, A., Kandalla, P. K., Marie, S., Di Santo, J., St Guily, J. L., Muntoni, F., Kim, J., Philippi, S., Spuler, S., Levy, N., Blumen, S. C., Voit, T., Wright, W. E., Aamiri, A., Butler-Browne, G. and Mouly, V. (2011) 'Immortalized pathological human myoblasts: towards a universal tool for the study of neuromuscular disorders.' Skelet Muscle, 1 2011/11/02, p. 34.

Lowell, B. (2005) 'Mitochondrial Dysfunction and Type 2 Diabetes'. Science, 307(5708) pp.384-387.

Oak, S., Tran, C., Pan, G., Thamotharan, M. and Devaskar, S. (2006) 'Perturbed skeletal muscle insulin signaling in the adult female intrauterine growth-restricted rat'. *American Journal of Physiology-Endocrinology and Metabolism*, 290(6) pp.E1321-E1330.

Floyd, Z., Trausch-Azar, J., Reinstein, E., Ciechanover, A. and Schwartz, A. (2001) 'The Nuclear Ubiquitin-Proteasome System Degrades MyoD'. *Journal of Biological Chemistry*, 276(25) pp.22468-22475.

Al-Shanti, N. and Stewart, C. (2008) 'PD98059 enhances C2 myoblast differentiation through p38 MAPK activation: a novel role for PD98059'. *Journal of Endocrinology*, 198(1) pp.243-252.

Saab, R. (2006) 'Pharmacologic inhibition of cyclin-dependent kinase 4/6 activity arrests proliferation in myoblasts and rhabdomyosarcoma-derived cells'. *Molecular Cancer Therapeutics*, 5(5) pp.1299-1308.

De Santa, F., Albini, S., Mezzaroma, E., Baron, L., Felsani, A. and Caruso, M. (2007) 'pRb-Dependent Cyclin D3 Protein Stabilization Is Required for Myogenic Differentiation'. *Molecular and Cellular Biology*, 27(20) pp.7248-7265.

Besson, A., Dowdy, S. and Roberts, J. (2008) 'CDK Inhibitors: Cell Cycle Regulators and Beyond'. *Developmental Cell*, 14(2) pp.159-169.

Ren, B. (2002) 'E2F integrates cell cycle progression with DNA repair, replication, and G2/M checkpoints'. *Genes & Development*, 16(2) pp.245-256.

De Falco, M. and De Luca, A. (2006) 'Involvement of cdks and cyclins in muscle differentiation.'. *European journal of histochemistry : EJH*, 50 1 pp.19-23.

Le Grand, F. and Rudnicki, M. (2007) 'Skeletal muscle satellite cells and adult myogenesis'. *Current Opinion in Cell Biology*, 19(6) pp.628-633.

Delaney-Sathy, L., Fessell, D., Jacobson, J. and Hayes, C. (2000) 'Sonography of Diabetic Muscle Infarction with MR Imaging, CT, and Pathologic Correlation'. *American Journal of Roentgenology*, 174(1) pp.165-169.

Ahmad, S., Khan, M., Akhter, F., Khan, M., Khan, A., Ashraf, J., Pandey, R. and Shahab, U. (2014) 'Glycoxidation of biological macromolecules: A critical approach to halt the menace of glycation'. *Glycobiology*, 24(11) pp.979-990.
Andersen, H. (2009) 'Motor function in diabetic neuropathy'. *Acta Neurologica Scandinavica*, 100(4) pp.211-220.

Picard, M., White, K. and Turnbull, D. (2013) 'Mitochondrial morphology, topology, and membrane interactions in skeletal muscle: a quantitative three-dimensional electron microscopy study'. *Journal of Applied Physiology*, 114(2) pp.161-171.

Kalyani, R., Metter, E., Egan, J., Golden, S. and Ferrucci, L. (2014) 'Hyperglycemia Predicts Persistently Lower Muscle Strength With Aging'. *Diabetes Care*, 38(1) pp.82-90.

Kalyani, R., Saudek, C., Brancati, F. and Selvin, E. (2010) 'Association of Diabetes, Comorbidities, and A1C With Functional Disability in Older Adults: Results from the National Health and Nutrition Examination Survey (NHANES), 1999-2006'. *Diabetes Care*, 33(5) pp.1055-1060.

Said, G. (2007) 'Diabetic neuropathy—a review'. *Nature Clinical Practice Neurology*, 3(6) pp.331-340.

Ramji, N., Toth, C., Kennedy, J. and Zochodne, D. (2007) 'Does diabetes mellitus target motor neurons?'. *Neurobiology of Disease*, 26(2) pp.301-311.

Gumy, L., Bampton, E. and Tolkovsky, A. (2008) 'Hyperglycaemia inhibits Schwann cell proliferation and migration and restricts regeneration of axons and Schwann cells from adult murine DRG'. *Molecular and Cellular Neuroscience*, 37(2) pp.298-311.

Allen, M., Doherty, T., Rice, C. and Kimpinski, K. (2016) 'Physiology in Medicine: neuromuscular consequences of diabetic neuropathy'. *Journal of Applied Physiology*, 121(1) pp.1-6.

Chiu, C., Yang, R., Sheu, M., Chan, D., Yang, T., Tsai, K., Chiang, C. and Liu, S. (2015) 'Advanced glycation end-products induce skeletal muscle atrophy and dysfunction in diabetic mice via a RAGE-mediated, AMPK-down-regulated, Akt pathway'. *The Journal of Pathology*, 238(3) pp.470-482.

Ashraf, J., Ahmad, S., Rabbani, G., Jan, A., Lee, E., Khan, R. and Choi, I. (2014) 'Physicochemical analysis of structural alteration and advanced glycation end products generation during glycation of H2A histone by 3-deoxyglucosone'. *IUBMB Life*, 66(10) pp.686-693.

Ashraf, J., Ahmad, S., Rabbani, G., Hasan, Q., Jan, A., Lee, E., Khan, R., Alam, K. and Choi, I. (2015) '3-Deoxyglucosone: A Potential Glycating Agent Accountable for Structural Alteration in H3 Histone Protein through Generation of Different AGEs'. *PLOS ONE*, 10(2) p.e0116804.

Ashraf, J., Ansari, M., Khan, H., Alzohairy, M. and Choi, I. (2016) 'Green synthesis of silver nanoparticles and characterization of their inhibitory effects on AGEs formation using biophysical techniques'. *Scientific Reports*, 6(1).

Ahmed, N. and Thornalley, P. (2007). Advanced glycation endproducts: what is their relevance to diabetic complications?. *Diabetes, Obesity and Metabolism*, 9(3), pp.233-245.

BEISSWENGER, B., DELUCIA, E., LAPOINT, N., SANFORD, R. and BEISSWENGER, P. (2005) 'Ketosis Leads to Increased Methylglyoxal Production on the Atkins Diet'. *Annals of the New York Academy of Sciences*, 1043(1) pp.201-210.

Vlassara, H. and Palace, M. (2002) 'Diabetes and advanced glycation endproducts'. *Journal of Internal Medicine*, 251(2) pp.87-101.

de M. Bandeira, S., da Fonseca, L., da S. Guedes, G., Rabelo, L., Goulart, M. and Vasconcelos, S. (2013) 'Oxidative Stress as an Underlying Contributor in the Development of Chronic Complications in Diabetes Mellitus'. *International Journal of Molecular Sciences*, 14(2) pp.3265-3284.

Ramasamy, R., Yan, S. and Schmidt, A. (2005) 'The RAGE Axis and Endothelial Dysfunction: Maladaptive Roles in the Diabetic Vasculature and Beyond'. *Trends in Cardiovascular Medicine*, 15(7) pp.237-243.

Ramasamy, R., Vannucci, S., Yan, S., Herold, K., Yan, S. and Schmidt, A. (2005). Advanced glycation end products and RAGE: a common thread in aging, diabetes, neurodegeneration, and inflammation. *Glycobiology*, 15(7), pp.16R-28R.

Kim, W., Hudson, B., Moser, B., Guo, J., Rong, L., Lu, Y., Qu, W., Lalla, E., Lerner, S., Chen, Y., Yan, S., D'agati, V., Naka, Y., Ramasamy, R., Herold, K., Yan, S. And Schmidt, A. (2005) 'Receptor For Advanced Glycation End Products And Its Ligands: A Journey From The Complications Of Diabetes To Its Pathogenesis'. *Annals of the New York Academy of Sciences*, 1043(1) pp.553-561.

Singh, V., Bali, A., Singh, N. and Jaggi, A. (2014) 'Advanced Glycation End Products and Diabetic Complications'. *The Korean Journal of Physiology & Pharmacology*, 18(1) p.1.

Snow, L., Fugere, N. and Thompson, L. (2007) 'Advanced Glycation End-Product Accumulation and Associated Protein Modification in Type II Skeletal Muscle With Aging'. *The Journals of Gerontology Series A: Biological Sciences and Medical Sciences*, 62(11) pp.1204-1210.

Cassese, A., Esposito, I., Fiory, F., Barbagallo, A., Paturzo, F., Mirra, P., Ulianich, L., Giacco, F., Iadicicco, C., Lombardi, A., Oriente, F., Van Obberghen, E., Beguinot, F., Formisano, P. and Miele, C. (2008). In Skeletal Muscle Advanced Glycation End Products (AGEs) Inhibit Insulin Action and Induce the Formation of Multimolecular Complexes Including the Receptor for AGEs. *Journal of Biological Chemistry*, 283(52), pp.36088-36099.

Uribarri, J., Cai, W., Ramdas, M., Goodman, S., Pyzik, R., Chen, X., Zhu, L., Striker, G. and Vlassara, H. (2011). Restriction of Advanced Glycation End Products Improves Insulin Resistance in Human Type 2 Diabetes: Potential role of AGER1 and SIRT1. *Diabetes Care*, 34(7), pp.1610-1616.

Ramamurthy, B. and Larsson, L. (2013). Detection of an aging-related increase in advanced glycation end products in fast- and slow-twitch skeletal muscles in the rat. *Biogerontology*, 14(3), pp.293-301.

Snow, L. and Thompson, L. (2009). Influence of Insulin and Muscle Fiber Type in Nε-(Carboxymethyl)-Lysine Accumulation in Soleus Muscle of Rats with Streptozotocin-Induced Diabetes Mellitus. *Pathobiology*, 76(5), pp.227-234.

Chiu, C.-Y., Yang, R.-S., Sheu, M.-L., Chan, D.-C., Yang, T.-H., Tsai, K.-S., Chiang, C.-K. and Liu, S.-H. (2016) 'Advanced glycation end-products induce skeletal muscle atrophy and dysfunction in diabetic mice via a RAGE-mediated, AMPK-down-regulated, Akt pathway: AGEs inhibition alleviates diabetic myopathy in mice.' *The Journal of Pathology*, 238(3) pp. 470-482.

Dalal, M., Ferrucci, L., Sun, K., Beck, J., Fried, L. and Semba, R. (2009). Elevated Serum Advanced Glycation End Products and Poor Grip Strength in Older Community-Dwelling Women. *The Journals of Gerontology Series A: Biological Sciences and Medical Sciences*, 64A(1), pp.132-137.

Sango, K., Mizukami, H., Horie, H. and Yagihashi, S. (2017). Impaired Axonal Regeneration in Diabetes. Perspective on the Underlying Mechanism from In Vivo and In Vitro Experimental Studies. *Frontiers in Endocrinology*, 8.

Sugimoto, K., Yasujima, M. and Yagihashi, S. (2008). Role of Advanced Glycation End Products in Diabetic Neuropathy. *Current Pharmaceutical Design*, 14(10), pp.953-961.

Semba, R., Nicklett, E. and Ferrucci, L. (2010). Does Accumulation of Advanced Glycation End Products Contribute to the Aging Phenotype?. *The Journals of Gerontology Series A: Biological Sciences and Medical Sciences*, 65A(9), pp.963-975.

Zeeshan, A., Chandrasekera, C. and Pippin, J. (2018).). Animal research for type 2 diabetes mellitus, its limited translation for clinical benefit, and the way forward. Alternatives to laboratory animals. *Alternatives to laboratory animals: ATLA*, 46(1), pp.13-22.

Furman, B. (2015). Streptozotocin-Induced Diabetic Models in Mice and Rats. *Current Protocols in Pharmacology*, pp.5.47.1-5.47.20.

King, A. (2012). The use of animal models in diabetes research. *British Journal of Pharmacology*, 166(3), pp.877-894.

Chandrasekera, P. (2014). Of rodents and men: Species-specific glucose regulation and type 2 diabetes research. *ALTEX*, pp.157-176.

Dyck, P., Albers, J., Andersen, H., Arezzo, J., Biessels, G., Bril, V., Feldman, E., Litchy, W., O'Brien, P. and Russell, J. (2011). Diabetic polyneuropathies: update on research definition, diagnostic criteria and estimation of severity. *Diabetes/Metabolism Research and Reviews*, 27(7), pp.620-628.

Souayah, N., Potian, J., Garcia, C., Krivitskaya, N., Boone, C., Routh, V. and McArdle, J. (2009). Motor unit number estimate as a predictor of motor dysfunction in an animal model of type 1 diabetes. *American Journal of Physiology-Endocrinology and Metabolism*, 297(3), pp.E602-E608.

Wilson, N. and Wright, D. (2014). Experimental motor neuropathy in diabetes. *Diabetes and the Nervous System*, pp.461-467.

POWER, G., DALTON, B., BEHM, D., VANDERVOORT, A., DOHERTY, T. and RICE, C. (2010). Motor Unit Number Estimates in Masters Runners. *Medicine & Science in Sports & Exercise*, 42(9), pp.1644-1650.

Wang, X., Chen, L., Liu, W., Su, B. and Zhang, Y. (2014). *Early Detection of Atrophy of Foot Muscles in Chinese Patients of Type 2 Diabetes Mellitus by High-Frequency Ultrasonography*.

Tiryaki, E. and Horak, H. (2014). ALS and Other Motor Neuron Diseases. *CONTINUUM: Lifelong Learning in Neurology*, 20, pp.1185-1207.

Gonzalez-Freire, M., de Cabo, R., Studenski, S. and Ferrucci, L. (2014). The Neuromuscular Junction: Aging at the Crossroad between Nerves and Muscle. *Frontiers in Aging Neuroscience*, 6.

Callaghan, B., Cheng, H., Stables, C., Smith, A. and Feldman, E. (2012). Diabetic neuropathy: clinical manifestations and current treatments. *The Lancet Neurology*, 11(6), pp.521-534.

Deshmukh, A. (2016) 'Insulin-stimulated glucose uptake in healthy and insulin-resistant skeletal muscle'. *Hormone Molecular Biology and Clinical Investigation*, 26(1).

Jensen, J., Rustad, P., Kolnes, A. and Lai, Y. (2011) 'The Role of Skeletal Muscle Glycogen Breakdown for Regulation of Insulin Sensitivity by Exercise'. *Frontiers in Physiology*, 2.

Demestre, M., Orth, M., Föhr, K. J., Achberger, K., Ludolph, A. C., Liebau, S. and Boeckers, T. M. (2015) 'Formation and characterisation of neuromuscular junctions between hiPSC derived motor neurons and myotubes.' *Stem Cell Research*, 15(2), pp. 328-336.

Umbach, J. A., Adams, K. L., Gundersen, C. B. and Novitch, B. G. (2012) 'Functional Neuromuscular Junctions Formed by Embryonic Stem Cell-Derived Motor Neurons.' *PLoS ONE*, 7(5), p. e36049.

Harper, J. M., Krishnan, C., Darman, J. S., Deshpande, D. M., Peck, S., Shats, I., Backovic, S., Rothstein, J. D. and Kerr, D. A. (2004) 'Axonal growth of embryonic stem cell-derived motor neurons in vitro and in motoneuron-injured adult rats.' *Proc Natl Acad Sci U S A*, 101(18), pp. 7123-7128.

Guo, X., Greene, K., Akanda, N., Smith, A., Stancescu, M., Lambert, S., Vandenburgh, H. and Hickman, J. (2014) 'In vitro Differentiation of Functional Human Skeletal Myotubes in a Defined System.' *Biomater Sci*, 2(1), pp. 131-138.

Arnold, A.-S., Christe, M. and Handschin, C. (2012) 'A Functional Motor Unit in the Culture Dish: Coculture of Spinal Cord Explants and Muscle Cells.' *Journal of Visualized Experiments : JoVE*, (62),p. 3616.

Mouly, V., Aamiri, A., Perie, S., Mamchaoui, K., Barani, A., Bigot, A., Bouazza, B., Francois, V., Furling, D., Jacquemin, V., Negroni, E., Riederer, I., Vignaud, A., St Guily, J. L. and Butler-Browne, G. S. (2005) 'Myoblast transfer therapy: is there any light at the end of the tunnel?' *Acta Myol*, 24(2), pp. 128-133.

Stockmann, M., Linta, L., Fohr, K. J., Boeckers, A., Ludolph, A. C., Kuh, G. F., Udvardi, P. T., Proepper, C., Storch, A., Kleger, A., Liebau, S. and Boeckers, T. M. (2013) 'Developmental and functional nature of human iPSC derived motor neurons.' *Stem Cell Rev*, 9(4), pp. 475-492.

Rumsey, J. W., Das, M., Stancescu, M., Bott, M., Fernandez-Valle, C. and Hickman, J. J. (2009) 'Node of Ranvier Formation on Motor neurons In Vitro.' *Biomaterials*, 30(21), pp. 3567-3572.

Calcutt, N., Cooper, M., Kern, T. and Schmidt, A. (2009) 'Therapies for hyperglycaemia-induced diabetic complications: from animal models to clinical trials'. *Nature Reviews Drug Discovery*, 8(5) pp.417-430.

Kawser Hossain, M., Abdal Dayem, A., Han, J., Kumar Saha, S., Yang, G., Choi, H. and Cho, S. (2016) 'Recent Advances in Disease Modeling and Drug Discovery for Diabetes Mellitus Using Induced Pluripotent Stem Cells'. *International Journal of Molecular Sciences*, 17(2) p.256.

Jang, J., Yoo, J., Lee, J., Lee, D., Kim, J., Huh, Y., Kim, D., Park, C., Hwang, D., Kim, H., Kang, H. and Kim, D. (2012) 'Disease-specific induced pluripotent stem cells: a platform for human disease modeling and drug discovery'. *Experimental & Molecular Medicine*, 44(3) p.202.

Chun, Y., Chaudhari, P. and Jang, Y. (2010) 'Applications of Patient-Specific Induced Pluripotent Stem Cells; Focused on Disease Modeling, Drug Screening and Therapeutic Potentials for Liver Disease'. *International Journal of Biological Sciences*, pp.796-805.

Haase, G. (2006) 'Motor Neuron Diseases: Cellular and Animal Models.' *In Reviews in Cell Biology and Molecular Medicine*. Wiley-VCH Verlag GmbH & Co.

Prather, R. S., Lorson, M., Ross, J. W., Whyte, J. J. and Walters, E. (2013) 'Genetically Engineered Pig Models for Human Diseases.' *Annual review of animal biosciences*, 1, 01/03, pp. 203-219.

Suuronen, E. J., McLaughlin, C. R., Stys, P. K., Nakamura, M., Munger, R. and Griffith, M. (2004) 'Functional Innervation in Tissue Engineered Models for In Vitro Study and Testing Purposes.' *Toxicological Sciences*, 82(2) pp. 525-533.

Schneider, C., Rasband, W. and Eliceiri, K. (2012) 'NIH Image to ImageJ: 25 years of image analysis'. *Nature Methods*, 9(7) pp.671-675.

Ren, K., Crouzier, T., Roy, C. and Picart, C. (2008) 'Polyelectrolyte multilayer films of controlled stiffness modulate myoblast cells differentiation.' *Adv Funct Mater*, 18(9) pp. 1378-1389.

Ricotti, L., Taccola, S., Bernardeschi, I., Pensabene, V., Dario, P. and Menciassi, A. (2011) 'Quantification of growth and differentiation of C2C12 skeletal muscle cells on PSS-PAH-based polyelectrolyte layer-by-layer nanofilms.' *Biomed Mater*, 6(3), Jun, p. 031001.

Grubisic, V., Gottipati, M. K., Stout, R. F., Jr., Grammer, J. R. and Parpura, V. (2014) 'Heterogeneity of myotubes generated by the MyoD and E12 basic helix-loop-helix transcription factors in otherwise non-differentiation growth conditions.' *Biomaterials*, 35(7), Feb, pp. 2188-2198.

Al-Dabbagh, S., McPhee, J. S., Murgatroyd, C., Butler-Browne, G., Stewart, C. E. and Al-Shanti, N. (2015) 'The lymphocyte secretome from young adults enhances skeletal muscle proliferation and migration, but effects are attenuated in the secretome of older adults ' *Physiological Reports*, 3(8) p. e12518.

Copeland, R., Bullen, J. and Hart, G. (2008) 'Cross-talk between GlcNAcylation and phosphorylation: roles in insulin resistance and glucose toxicity'. *American Journal of Physiology-Endocrinology and Metabolism*, 295(1) pp.E17-E28.

Yaturu, S. (2011) 'Obesity and type 2 diabetes'. *Journal of Diabetes Mellitus*, 01(04) pp.79-95.

Grabiec, K., Gajewska, M., Milewska, M., Błaszczyk, M. and Grzelkowska-Kowalczyk, K. (2014) 'The influence of high glucose and high insulin on mechanisms controlling cell cycle progression and arrest in mouse C2C12 myoblasts: the comparison with IGF-I effect'. *Journal of Endocrinological Investigation*, 37(3) pp.233-245.

Hunt, L., Xu, B., Finkelstein, D., Fan, Y., Carroll, P., Cheng, P., Eisenman, R. and Demontis, F. (2015) 'The glucose-sensing transcription factor MLX promotes myogenesis via myokine signaling'. *Genes & Development*, 29(23) pp.2475-2489.

Howard, A., McNeil, A., Xiong, F., Xiong, W. and McNeil, P. (2011) 'A Novel Cellular Defect in Diabetes'. *Diabetes*, 60(11) pp.3034-3043.

Nedachi, T., Kadotani, A., Ariga, M., Katagiri, H. and Kanzaki, M. (2008) 'Ambient glucose levels qualify the potency of insulin myogenic actions by regulating SIRT1 and FoxO3a in C2C12 myocytes'. *American Journal of Physiology-Endocrinology and Metabolism*, 294(4) pp.E668-E678.

Grzelkowska-Kowalczyk, K. (2014) 'The Effect of High Glucose on Mechanisms Controlling Proliferation of Mouse C2C12 Myoblasts'. *International Journal of Diabetes & Clinical Diagnosis*, 1(1).

Grzelkowska-Kowalczyk, K., Wieteska-Skrzeczyńska, W., Grabiec, K. and Tokarska, J. (2012) 'High glucose-mediated alterations of mechanisms important in myogenesis of mouse C2C12 myoblasts'. *Cell Biology International*, 37(1) pp.29-35.

Cassese, A., Esposito, I., Fiory, F., Barbagallo, A., Paturzo, F., Mirra, P., Ulianich, L., Giacco, F., Iadicicco, C., Lombardi, A., Oriente, F., Van Obberghen, E., Beguinot, F., Formisano, P. and Miele, C. (2008) 'In Skeletal Muscle Advanced Glycation End Products (AGEs) Inhibit Insulin Action and Induce the Formation of Multimolecular Complexes Including the Receptor for AGEs'. *Journal of Biological Chemistry*, 283(52) pp.36088-36099.

Riuzzi, F., Sorci, G., Sagheddu, R. and Donato, R. (2012) 'HMGB1-RAGE regulates muscle satellite cell homeostasis through p38-MAPK- and myogenin-dependent repression of Pax7 transcription'. *Journal of Cell Science*, 125(6) pp.1440-1454.

Folker, E. and Baylies, M. (2013) 'Nuclear positioning in muscle development and disease'. *Frontiers in Physiology*, 4.

Jungbluth, H. and Gautel, M. (2014) 'Pathogenic Mechanisms in Centronuclear Myopathies'. *Frontiers in Aging Neuroscience*, 6.

Tasfaout, H., Cowling, B. and Laporte, J. (2018) 'Centronuclear myopathies under attack: A plethora of therapeutic targets'. *Journal of Neuromuscular Diseases*, pp.1-20.

Roman, W. and Gomes, E. (2017) 'Nuclear positioning in skeletal muscle'. *Seminars in Cell & Developmental Biology*.

Folker, E. and Baylies, M. (2013) 'Nuclear positioning in muscle development and disease'. *Frontiers in Physiology*, 4.

Cadot, B., Gache, V. and Gomes, E. (2015) 'Moving and positioning the nucleus in skeletal muscle – one step at a time'. *Nucleus*, 6(5) pp.373-381.

Romero, N. and Bitoun, M. (2011) 'Centronuclear Myopathies'. *Seminars in Pediatric Neurology*, 18(4) pp.250-256.

Drenth, H., Zuidema, S., Bunt, S., Bautmans, I., van der Schans, C. and Hobbelen, H. (2016) 'The Contribution of Advanced Glycation End product (AGE) accumulation to the decline in motor function'. *European Review of Aging and Physical Activity*, 13(1).

Xing, Y. and Zhang, X. (2013) 'Injury of Cortical Neurons Is Caused by the Advanced Glycation End Products-Mediated Pathway.'. *Neural Regeneration Research*, 8.10 pp.909–915.

Zochodne, D., Ramji, N. and Toth, C. (2008) 'Neuronal Targeting in Diabetes Mellitus: A Story of Sensory Neurons and Motor Neurons'. *The Neuroscientist*, 14(4) pp.311-318.

Sango, K., Mizukami, H., Horie, H. and Yagihashi, S. (2017) 'Impaired Axonal Regeneration in Diabetes. Perspective on the Underlying Mechanism from In Vivo and In Vitro Experimental Studies'. *Frontiers in Endocrinology*, 8.

King, R. (2001) 'The role of glycation in the pathogenesis of diabetic polyneuropathy.'. *Molecular Pathology*, (54(6) pp.400–408.

Edwards, J., Vincent, A., Cheng, H. and Feldman, E. (2008) 'Diabetic neuropathy: Mechanisms to management'. *Pharmacology & Therapeutics*, 120(1) pp.1-34.

Ahmed, N. (2005) 'Advanced glycation endproducts—role in pathology of diabetic complications'. *Diabetes Research and Clinical Practice*, 67(1) pp.3-21.

Öztürk, G., Şekeroğlu, M., Erdoğan, E. and Öztürk, M. (2006) 'The effect of non-enzymatic glycation of extracellular matrix proteins on axonal regeneration in vitro'. *Acta Neuropathologica*, 112(5) pp.627-632.

Trnková, L., Dršata, J. and Boušová, I. (2015) 'Oxidation as an important factor of protein damage: Implications for Maillard reaction'. *Journal of Biosciences*, 40(2) pp.419-439.

Muramatsu, K., Niwa, M., Nagai, M., Kamimura, T., Sasaki, S. and Ishiguro, T. (2012) 'The size of motor neurons of the gastrocnemius muscle in rats with diabetes'. *Neuroscience Letters*, 531(2) pp.109-113.

Souayah, N., Potian, J., Garcia, C., Krivitskaya, N., Boone, C., Routh, V. and McArdle, J. (2009) 'Motor unit number estimate as a predictor of motor dysfunction in an animal model of type 1 diabetes'. *American Journal of Physiology-Endocrinology and Metabolism*, 297(3) pp.E602-E608.

Höke, A. (2012) 'Animal Models of Peripheral Neuropathies'. *Neurotherapeutics*, 9(2) pp.262-269.

Brand, Martin D., and David G. Nicholls. "Assessing Mitochondrial Dysfunction in Cells." *Biochemical Journal* 435.2 (2011): pp. 297-312.

Porter, R. (2001) 'Mitochondrial proton leak: a role for uncoupling proteins 2 and 3?'. *Biochimica et Biophysica Acta (BBA) - Bioenergetics*, 1504(1) pp.120-127.

Sansbury, B., Riggs, D., Brainard, R., Salabei, J., Jones, S. and Hill, B. (2011) 'Responses of hypertrophied myocytes to reactive species: implications for glycolysis and electrophile metabolism'. *Biochemical Journal*, 435(2) pp.519-528.

Dranka, B., Benavides, G., Diers, A., Giordano, S., Zelickson, B., Reily, C., Zou, L., Chatham, J., Hill, B., Zhang, J., Landar, A. and Darley-Usmar, V. (2011) 'Assessing bioenergetic function in response to oxidative stress by metabolic profiling'. *Free Radical Biology and Medicine*, 51(9) pp.1621-1635.

Hill, B., Benavides, G., Lancaster, J., Ballinger, S., Dell'Italia, L., Zhang, J. and Darley-Usmar, V. (2012) 'Integration of cellular bioenergetics with mitochondrial quality control and autophagy'. *Biological Chemistry*, 393(12).

Leinninger, G., Edwards, J., Lipshaw, M. and Feldman, E. (2006) 'Mechanisms of Disease: mitochondria as new therapeutic targets in diabetic neuropathy'. *Nature Clinical Practice Neurology*, 2(11) pp.620-628.

Brownlee, M. (2001) 'Biochemistry and molecular cell biology of diabetic complications'. *Nature*, 414(6865) pp.813-820.

Wada, R., Nishizawa, Y., Yagihashi, N., Takeuchi, M., Ishikawa, Y., Yasumura, K., Nakano, M. and Yagihashi, S. (2001) 'Effects of OPB-9195, anti-glycation agent, on experimental diabetic neuropathy'. *European Journal of Clinical Investigation*, 31(6) pp.513-520.

Ilnytska, O., Lyzogubov, V., Stevens, M., Drel, V., Mashtalir, N., Pacher, P., Yorek, M. and Obrosova, I. (2006) 'Poly(ADP-Ribose) Polymerase Inhibition Alleviates Experimental Diabetic Sensory Neuropathy'. *Diabetes*, 55(6) pp.1686-1694.

Vincent, A. and Feldman, E. (2004) 'New Insights into the Mechanisms of Diabetic Neuropathy'. *Reviews in Endocrine and Metabolic Disorders*, 5(3) pp.227-236.